TABLE 2. Treatment-Related Death and Its Cumulative Incidence

Characteristics	Chemotherapy Alone[a] (n = 927)	Concurrent Chemoradiotherapy (n = 245)	Radiotherapy Alone[a] (n = 96)
No. of treatment-related deaths	7	12	4
Cumulative incidence (%)	0.8	4.9	4.2
Sex			
Male	5	11	4
Female	2	1	0
Age of patients who died of treatment (yr)			
Median (range)	69 (46–77)	68 (50–77)	75 (65–77)
Causes			
Treatment-induced lung injury	4	11	4
Infectious pneumonia	2	1	0
Unknown	1	0	0
Chemotherapy regimen			
Platinum + taxane	2	2	—
EGFR-TKI	4	—	—
Platinum + antimetabolite	1	—	—
Platinum + etoposide	0	1	—
Platinum + vinca alkaloid	0	8	—
Others	0	1	—

[a] Forty-three patients who received sequential chemotherapy followed by radiotherapy are included in the analysis of both the chemotherapy-alone group and radiotherapy-alone group, as described in the text.

EGFR-TKI, epidermal growth factor receptor-tyrosine kinase inhibitor.

related deaths occurred in 4 of 96 (4.2%) patients: all 4 (4.2%) patients died of radiation pneumonitis.

Risk Factors for TRD from Chemotherapy

Statistically significant factors identified by the univariate analysis were a performance status of 2 to 4, hypoxia, hypoalbuminemia, hyponatremia, out of clinical trials, and treatment with epidermal growth factor receptor-tyrosine kinase inhibitors (EGFR-TKIs) (Table 3). Although statistically significant, the degrees of hyponatremia in the events were neither clinically significant nor symptomatic for the range of 133 to 137 mEq/L. Pulmonary fibrosis and emphysema were noted in 34 and 69 patients, respectively, among the 927 patients. None of these patients with lung disease died of treatment in this study. Multivariate analysis was not performed because the number of observed events was too small (n = 7).

Risk Factors for TRD from Concurrent Chemoradiotherapy

None of the factors, except for pulmonary fibrosis, were found to be statistically significant in the univariate analysis, although a trend toward increase in the risk of TRD was observed in patients of advanced age (>70 years) and with lower lobe as the primary tumor site (Table 4). Pulmonary fibrosis appeared to be a statistically significant risk factor for TRD; however, it was excluded from the multivariate analysis because of its limited incidence. Thus, we did not perform multivariate analysis for chemoradiotherapy group, and an analysis of the risk of TRD associated with thoracic radiotherapy alone was not conducted because of the limited number of cases.

DISCUSSION

We identified a total of 23 TRDs out of the 1225 patients (1.9%) enrolled in this study, which is lower than the rate (2.7%) indicated in a previous report, particularly in relation to the number of TRDs from infections, including pneumonia and sepsis.[1] The reason for the decrease in the incidence of infection-related deaths is likely explained by the infrequent use of triplet regimens when compared with previous studies. Especially, mitomycin-C-containing regimens are regarded as effective regimens in the treatment of lung cancer; however, prolonged neutropenia has been observed with these regimens. Ohe et al.[1] reported that combined mitomycin-C + vindesine + CDDP (MVP regimen) therapy is a risk factor for chemotherapy-related TRD (toxic deaths occurred in 9 of 301 patients; odds ratio [OR] = 9.36, 95% confidence interval [CI] = 1.29–68.0, p = 0.027). In this study, only 35 patients, the majority (89%) of whom were enrolled in a clinical trial, received the MVP regimen. In the past, however, the MVP regimen was widely used as part of practice-based regimens (only 28% recorded under clinical trials). In most cases, patients who were not eligible for clinical trials ended up receiving the MVP regimen. Another reason is the relatively frequent use of EGFR-TKI (in 13.5% of the patients in this study) at present, which does not induce myelosuppression. The reduction in the frequency of TRD might also be explained by a progress in supportive care in the treatments given for cancer treatment toxicities.

This study revealed that drug-induced lung injury was the most frequent cause of TRD in the era of molecular-targeted therapy. Three (75%) of four TRDs from drug-induced lung injury were associated with gefitinib. The re-

TABLE 3. Risk Factors for Treatment-Related Death from Chemotherapy

Factors	No. of Patients	Cumulative Incidence (%)	Univariate Analysis OR (95% CI)	*p*
Sex				
Female	288	0.8	1	
Male	639	0.7	1.13 (0.22–5.76)	0.89
Age				
<70	689	0.6	1	
≥70	238	1.3	2.17 (0.51–9.30)	0.30
PS				
0–1	870	0.5	1	
2–4	57	5.2	11.4 (3.53–37.1)	<0.001
Smoking history				
No	271	0.4	1	
Yes	656	0.9	2.49 (0.30–20.8)	0.40
PaO_2 (Torr)				
≥70	812	0.2	1	
<70	105	4.8	19.3 (6.06–61.7)	<0.001
Hemoglobin (g/dl)				
≥13.7	371	0.5	1	
<13.7	556	0.9	1.67 (0.33–8.39)	0.54
Albumin (g/dl)				
≥3.7	663	0.3	1	
<3.7	264	1.9	6.28 (1.51–26.1)	0.012
AST (IU/L)				
≤33	831	0.6	1	
>33	96	2.1	3.46 (0.75–16.0)	0.11
Na (mEq/L)				
≥138	819	0.1	1	
<138	108	5.6	45.5 (13.4–154)	<0.001
Clinical trial				
No	355	1.7	1	
Yes	572	0.2	0.10 (0.58–0.019)	0.001
Platinum + taxane				
No	559	0.9	1	
Yes	368	0.5	0.61 (0.12–3.14)	0.55
EGFR-TKIs				
No	802	0.4	1	
Yes	125	3.2	8.56 (2.48–29.5)	0.001
Platinum + antimetabolite				
No	842	0.7	1	
Yes	85	1.1	1.66 (0.20–13.9)	0.64

Multivariate analysis was not performed because the number of observed events was too small ($n = 7$).

OR, odds ratio; CI, confidence interval; PS, performance status; AST, aspartate transaminase; EGFR-TKIs, epidermal growth factor receptor-tyrosine kinase inhibitors.

TABLE 4. Risk Factors for Treatment-Related Death from Concurrent Chemoradiotherapy

Factors	No. of Patients	Cumulative Incidence (%)	Univariate Analysis OR (95% CI)	*p*
Sex				
Female	44	2.3	1	
Male	201	5.2	2.41 (0.35–16.6)	0.37
Age (yr)				
<70	221	4.1	1	
≥70	24	12.5	3.07 (0.92–10.3)	0.069
PS				
0	114	5.3	1	
1	131	4.6	0.87 (0.29–2.62)	0.81
Smoking history				
No	32	3.2	1	
Yes	213	5.2	1.65 (0.23–11.9)	0.24
Fibrosis				
No	244	4.5	1	
Yes	1	100	22.2 (5.61–87.8)	<0.001
Emphysema				
No	215	4.7	1	
Yes	30	6.7	1.43 (0.33–6.25)	0.63
Location of the tumor				
Other lobes	189	3.7	1	
Lower lobe	56	8.9	2.41 (0.82–7.13)	0.11
Histology				
SCLC	54	1.9	1	
NSCLC	191	5.8	3.11 (0.47–20.6)	0.24
Hemoglobin (g/dl)				
≥13.7	146	4.1	1	
<13.7	99	6.1	1.48 (0.49–4.42)	0.48
Albumin (g/dl)				
≥3.7	198	4.5	1	
<3.7	47	6.4	1.40 (0.40–4.99)	0.6
Na (mEq/L)				
≥138	219	5.0	1	
<138	26	3.8	0.77 (0.11–5.60)	0.79
Clinical trial				
No	114	5.3	1	
Yes	131	4.6	0.87 (0.29–2.62)	0.81
Platinum + taxane				
No	224	4.5	1	
Yes	21	9.5	2.25 (0.46–11.0)	0.32
Platinum + vinca alkaloid				
No	77	5.2	1	
Yes	168	4.8	0.91 (0.27–3.13)	0.88

Multivariate analysis was not performed because only fibrosis was significant in univariate analysis.

OR, odds ratio; CI, confidence interval; PS, performance status; NSCLC, non-small cell lung cancer.

ported risk factors for interstitial lung disease in NSCLC patients treated with gefitinib are male sex, history of smoking, and underlying interstitial pneumonitis.[11] In this study, however, none of these factors were associated with TRD from chemotherapy. Another TRD from drug-induced lung injury occurred in a patient who received gemcitabine, but this patient was also free from underlying pulmonary disease or concomitant use of taxanes, which are reported to be risk factors for gemcitabine-associated interstitial lung disease.[12]

For patients who receive concurrent chemoradiotherapy, we would like to emphasize the previous finding that the

presence of evidence of pulmonary fibrosis on a plain chest x-ray is an extremely strong risk factor for TRD (OR = 166, 95% CI = 8.79–3122, $p < 0.001$).[1] In this study, only one patient with pulmonary fibrosis was identified, and pulmonary fibrosis was not included in the multivariate analysis because of the small number of patients with this factor, because we generally exclude patients with evidence of pulmonary fibrosis on the chest x-ray from consideration of concurrent chemoradiotherapy. This study also suggested that advanced age may be a risk factor for TRD. This is consistent with the results of previous studies.[1,13–15] The association between advanced age and fatal radiation-induced lung injury may be explained by the increased likelihood of these patients developing comorbid lung disease, particularly among patients with a history of heavy tobacco exposure. A meta-analysis of chemoradiotherapy using individual data from 1764 patients with locally advanced NSCLC showed that the benefit of chemoradiotherapy was obtained in elderly patients (≥71 years) as well as in younger patients. However, it might be assumed that patients who are included in such trials are fit patients with minimal comorbidities. In addition, despite the increase in toxicity that accompanied chemoradiotherapy in elderly patients, it seemed that they had disease control and survival rates similar to those of younger patients.[16]

In conclusion, TRD occurred in a total of 1.9% of patients and was caused in the majority of the cases by treatment-related lung injury. This finding is in clear contrast with previous reports which suggested that the principal cause of TRD in lung cancer patients was septic shock.

ACKNOWLEDGMENTS

The authors thank Ms. Mika Nagai for her assistance in the preparation of this manuscript.

REFERENCES

1. Ohe Y, Yamamoto S, Suzuki K, et al. Risk factors of treatment-related death in chemotherapy and thoracic radiotherapy for lung cancer. *Eur J Cancer* 2001;37:54–63.
2. Morittu L, Earl HM, Souhami RL, et al. Patients at risk of chemotherapy-associated toxicity in small cell lung cancer. *Br J Cancer* 1989;59: 801–804.
3. Radford JA, Ryder WD, Dodwell D, et al. Predicting septic complications of chemotherapy:an analysis of 382 patients treated for small cell lung cancer without dose reduction after major sepsis. *Eur J Cancer* 1992;29A:81–86.
4. Stephens RJ, Girling DJ, Machin D. Treatment-related deaths in small cell lung cancer trials: can patients at risk be identified? Medical Research Council Lung Cancer Working Party. *Lung Cancer* 1994;11: 259–274.
5. Sekine I, Noda K, Oshita F, et al. Phase I study of cisplatin, vinorelbine, and concurrent thoracic radiotherapy for unresectable stage III non-small cell lung cancer. *Cancer Sci* 2004;95:691–695.
6. Graham MV, Purdy JA, Emami B, et al. Clinical dose-volume histogram analysis for pneumonitis after 3D treatment for non-small cell lung cancer. *Int J Radiat Oncol Biol Phys* 1999;45:323–329.
7. Ohe Y, Ohashi Y, Kubota K, et al. Randomized phase III study of cisplatin plus irinotecan versus carboplatin plus paclitaxel, cisplatin plus gemcitabine, and cisplatin plus vinorelbine for advanced non-small-cell lung cancer: Four-Arm Cooperative Study in Japan. *Ann Oncol* 2007; 18:317–323.
8. Takada M, Fukuoka M, Kawahara M, et al. Phase III study of concurrent versus sequential thoracic radiotherapy in combination with cisplatin and etoposide for limited-stage small-cell lung cancer: results of the Japan Clinical Oncology Group Study 9104. *J Clin Oncol* 2002;20: 3054–3060.
9. Noda K, Nishiwaki Y, Kawahara M, et al; Japan Clinical Oncology Group. Irinotecan plus cisplatin compared with etoposide plus cisplatin for extensive small-cell lung cancer. *N Engl J Med* 2002;346:85–91.
10. Sekine I, Sumi M, Ito Y, et al. Retrospective analysis of steroid therapy for radiation-induced lung injury in lung cancer patients. *Radiother Oncol* 2006;80:93–97.
11. Ando M, Okamoto I, Yamamoto N, et al. Predictive factors for interstitial lung disease, antitumor response, and survival in non-small-cell lung cancer patients treated with gefitinib. *J Clin Oncol* 2006;24:2549–2556.
12. Barlési F, Villani P, Doddoli C, et al. Gemcitabine-induced severe pulmonary toxicity. *Fundam Clin Pharmacol* 2004;18:85–91.
13. Yuen AR, Zou G, Turrisi AT, et al. Similar outcome of elderly patients in intergroup trial 0096: cisplatin, etoposide, and thoracic radiotherapy administered once or twice daily in limited stage small cell lung carcinoma. *Cancer* 2000;89:1953–1960.
14. Schild SE, Stella PJ, Geyer SM, et al. North Central Cancer Treatment Group. The outcome of combined-modality therapy for stage III non-small-cell lung cancer in the elderly. *J Clin Oncol* 2003;21:3201–3206.
15. Schild SE, Stella PJ, Brooks BJ, et al. Results of combined-modality therapy for limited-stage small cell lung carcinoma in the elderly. *Cancer* 2005;103:2349–2354.
16. Aupérin A, Le Péchoux C, Pignon JP, et al; Meta-Analysis of Cisplatin/carboplatin based Concomitant Chemotherapy in non-small cell Lung Cancer (MAC3-LC) Group. Concomitant radio-chemotherapy based on platin compounds in patients with locally advanced non-small cell lung cancer (NSCLC): a meta-analysis of individual data from 1764 patients. *Ann Oncol* 2006;17:473–483.

Lung Cancer 72 (2011) 309–315

Contents lists available at ScienceDirect

Lung Cancer

journal homepage: www.elsevier.com/locate/lungcan

Frequent *ALK* rearrangement and TTF-1/p63 co-expression in lung adenocarcinoma with signet-ring cell component

Akihiko Yoshida[a,b], Koji Tsuta[a], Shun-ichi Watanabe[c], Ikuo Sekine[d], Masashi Fukayama[b], Hitoshi Tsuda[a], Koh Furuta[a], Tatsuhiro Shibata[e,*]

[a] *Clinical Laboratory Division, National Cancer Center Hospital, Japan*
[b] *Department of Pathology, University of Tokyo, Japan*
[c] *Thoracic Surgery Division, National Cancer Center Hospital, Japan*
[d] *Division of Internal Medicine and Thoracic Oncology, National Cancer Center Hospital, Japan*
[e] *Cancer Genomics Project, Center for Medical Genomics, National Cancer Center Research Institute, 5-1-1 Tsukiji, Chuo-ku, Tokyo 104-0045 Japan*

ARTICLE INFO

Article history:
Received 10 June 2010
Received in revised form 9 September 2010
Accepted 19 September 2010

Keywords:
Adenocarcinoma
Signet-ring cell
ALK translocation
Immunohistochemistry
Polymerase chain reaction
Fluorescence in situ hybridization

ABSTRACT

Primary adenocarcinoma with signet-ring cell component (Ad-SRCC) of the lung has been well characterized clinicopathologically and histologically, but their genetics has rarely been investigated. A recent report suggesting an association between Ad-SRCC and *EML4-ALK* fusion prompted us to undertake a histological, immunohistochemical, and molecular analysis of 10 cases of primary Ad-SRCC identified out of 699 lung adenocarcinomas (1.4%). Most of the Ad-SRCCs showed characteristic architectural as well as cytological features including cohesive clustering of signet-ring cells, a solid/acinar growth pattern, and alveolar filling at the tumor periphery. Diffuse co-expression of TTF-1 and p63 was observed in half of the Ad-SRCCs, and this immunoprofile has not been recognized previously. Four Ad-SRCCs (40%) harbored *ALK* translocations detected by reverse-transcriptase polymerase chain reaction, fluorescence in situ hybridization, and immunohistochemistry. One new *EML4-ALK* fusion variant was identified. One *ALK*-rearranged tumor showed focal squamous differentiation. None of the present Ad-SRCCs had *EGFR* or *KRAS* mutations, regardless of *ALK* status. This study successfully utilized tumor histology alone to identify a subset of adenocarcinomas showing a high rate of *ALK* translocation. The characteristic histology, immunoprofile, frequent *ALK* translocation, and total lack of *EGFR* or *KRAS* mutations, may suggest that Ad-SRCC forms a histologically/molecularly coherent subgroup of adenocarcinoma.

1. Introduction

Lung cancer is the leading cause of cancer death both in men and women worldwide. Surgery, chemotherapy, and radiation therapy are the standard therapeutic modalities [1], and the treatment of lung cancer has conventionally been dictated by histological classification and tumor stage [1,2]. In recent years, the classification of lung cancer has become refined by molecular genetic data, and this trend has important therapeutic implications, helping to guide clinicians to the optimal treatment for individual patients [3,4].

In 2007, Soda et al. [5] discovered a novel transforming fusion gene joining the echinoderm microtubule-associated protein-like 4 (*EML4*) and anaplastic lymphoma kinase (*ALK*) genes in a subset of non-small-cell lung carcinoma (NSCLC). The *EML4-ALK* fusion gene is formed by a small inversion within the short arm of chromosome 2, and the encoded protein, a chimera comprising the N-terminal part of EML4 and the intracellular catalytic domain of ALK, is expressed constitutively and dimerized without ligand stimulation [5]. The presence of the *EML4-ALK* fusion in NSCLCs was subsequently confirmed by other investigators worldwide [6–16]. A number of fusion variants have been identified to date, and another rare fusion partner for *ALK* is *KIF5B* [15]. Since ALK is a tyrosine kinase receptor, this subtype of NSCLC is expected to be a good candidate for treatment with small-molecule ALK tyrosine kinase inhibitors [2,17]. Several studies have already confirmed that such drugs induce growth cessation of *ALK*-translocation-positive NSCLC in vitro [5,10] and in xenografts [10,18]. A preliminary phase I study of one of such drugs yielded promising results in a cohort of patients with *ALK*-rearranged NSCLCs [19].

Signet-ring cell component in primary adenocarcinoma of the lung has been recognized for more than two decades [20]. The clinicopathological features of adenocarcinoma with signet-ring cell component (Ad-SRCC) have been well described in the literature [21,22], and its histological features repeatedly documented [21,23–25]. However, the genetic background of this subtype of adenocarcinoma has not been investigated in detail [24,26], and

* Corresponding author. Tel.: +81 3 3547 5201x3123; fax: +81 3 3547 5137.
E-mail address: tashibat@ncc.go.jp (T. Shibata).

0169-5002/$ – see front matter © 2010 Elsevier Ireland Ltd. All rights reserved.
doi:10.1016/j.lungcan.2010.09.013

there has been a paucity of comprehensive analyses of Ad-SRCCs covering both phenotypic and molecular genetic aspects. Recently, Rodig et al. [11] identified frequent signet-ring cell populations in 20 adenocarcinomas that carried *ALK*-rearrangement by fluorescence in situ hybridization (FISH) analysis. Prompted by this report, we examined 10 consecutive cases of surgically resected Ad-SRCCs of the lung. Along with a detailed histological study and standard *EGFR* and *KRAS* mutation assays, we investigated the *ALK* status of these tumors using multiplex reverse-transcription polymerase chain reaction (RT-PCR), FISH, and immunohistochemistry (IHC).

2. Materials and methods

2.1. Case selection

We reviewed 699 consecutive primary adenocarcinomas of the lung resected at the National Cancer Center (NCC), Tokyo, in 2004 and 2005, and retrieved cases of Ad-SRCC. The possibility of metastasis from other sites was clinically/radiologically excluded. The diagnosis of Ad-SRCC was based on the presence of signet-ring cells, which have marginally located crescentic nuclei and abundant intracytoplasmic mucin, the latter being highlighted dark blue by alcian blue- periodic acid-Schiff (AB-PAS) staining. We accepted tumors as Ad-SRCCs when unequivocal signet-ring cells accounted for ≥5% of the total tumor cells. This cutoff is chosen because there is no universally agreed upon threshold, and because routine histological examination can readily identify signet-ring cells when they occupy at least 5% of the tumor cells based on our experience and that of others [27]. The signet-ring cell percentage was calculated after reviewing all the available slides, which represented the entire lesion in small-sized tumors (3.0 cm or less), or the product of adequate sampling in larger tumors. Mucinous bronchioloalveolar carcinoma (BAC), colloid carcinoma, and solid adenocarcinoma with mucin production may contain variably shaped mucus cells [23,28], but they generally lack signet-ring cells ≥5% and are therefore differentiated from Ad-SRCC. Each adenocarcinoma was estimated for tumor size, percentage of signet-ring cells among total tumor cells, nuclear grade (low, intermediate, or high), TNM stage [29], and predominant growth pattern as defined by the World Health Organization (WHO) [1]. Clinical information for each case was collected by reviewing the medical records. This study was approved by the Institutional Review Board of NCC.

2.2. IHC

Four-micrometer-thick sections were deparaffinized. Heat-induced epitope retrieval was performed with 1.0-mmol/L citrate buffer (pH 6.0) for ALK protein and TTF-1, and with TRS9 (DAKO, Carpinteria, CA) for p63. The slides were treated with 3% hydrogen peroxide for 20 min. The slides were then incubated with primary antibodies against ALK protein (1:40, ALK1, DAKO), p63 (1:400, 4A4, DAKO), and TTF-1 (1:100, 8G7G3/1, DAKO) for 1 h at room temperature. Immunoreactions were detected using the Envison-plus system (DAKO) for p63 and TTF-1, and CSAII (DAKO) for ALK protein. The reactions were visualized with 3,3′-diaminobenzidine. Appropriate positive and negative controls were used. Only the nuclear stain was deemed positive for TTF-1 and p63, and the extent of staining was graded as 0 (0–10%), 1+ (>10–25%), 2+ (>25–50%), and 3+ (>50%). Strong diffuse granular cytoplasmic staining was regarded as positive for ALK.

2.3. FISH

FISH was performed on formalin-fixed, paraffin-embedded tumor tissues using a break-apart probe for the *ALK* gene (Vysis LSI ALK Dual Color, break-apart rearrangement probe; Abbott Molecular) in accordance with the manufacturer's instructions. Positive rearrangement was defined as a splitting apart of the fluorescence probes flanking the *ALK* locus. In addition, as recently shown by others in abstract form [30], loss of 5′ locus (green signal) of split-apart *ALK* was considered equivalent to the *ALK* rearrangement, likely reflecting the loss of non-functioning *ALK-EML4* fusion product. Three experienced observers independently assessed the slides. Adjacent uninvolved lung tissue was used as negative control. Decisions regarding positivity and negativity required unanimous agreement among three observers, and cases for which opinions were divided were designated indeterminate for *ALK* rearrangement.

Table 1
Primers used for RT-PCR and sequencing.

For detection of *EML4-ALK* fusion	
EA-F1	5′ GTGCAGTGTTTAGCATTCTTGGGG 3′
EA-F2	5′ AGCTACATCACACACCTTGACTGG 3′
EA-F3	5′ TACCAGTGCTGTCTCAATTGCAGG 3′
EA-F4	5′ GCTTTCCCCGCAAGATGGACGG 3′
ALK-R	5′ TCTTGCCAGCAAAGCAGTAGTTGG 3′
For detection of *KIF5B-ALK* fusion	
KA-F1	5′ CAGCTGAGAGAGTGAAAGCTTTGG 3′
KA-F2	5′ GACAGTTGGAGGAATCTGTCGATG 3′
KA-F3	5′ ATCCTGCGGAACACTATTCAGTGG 3′
KA-F4	5′ TCAAGCACATCTCAAGAGCAAGTG 3′
ALK-R	5′ TCTTGCCAGCAAAGCAGTAGTTGG 3′
For detection of *EGFR* mutation	
EGFR-RTF1	5′ CCTCTTACACCCAGTGGAGAAGC 3′
EGFR-RTR1	5′ CAGTTGAGCAGGTACTGGGAGCC 3′
EGFR-RTF2	5′ TCCTGGACTATGTCCGGGAACAC 3′
EGFR-RTR2	5′ AGGTCATCAACTCCCAAACGGTC 3′
For detection of *KRAS* mutation	
KRAS-RTF1	5′ AGAGAGGCCTGCTGAAAATGACTG 3′
KRAS-RTR1	5′ CCATAGGTACATCTTCAGAGTCC 3′

2.4. RT-PCR and sequencing for ALK fusions

Frozen tumor tissues were powdered by CP02 (Covaris, Woburn, MA) and sonicated using a Covaris S2 (Covaris). Total RNA was extracted using a mirVana RNA Isolation Kit (Ambion, Foster City, CA). cDNA was synthesized with MMTV reverse transcriptase (Transcriptor First Strand cDNA Synthesis Kit, Roche Diagnostics, Switzerland). To amplify *ALK* fusion genes, a mixture of primers covering potential breakpoints of fusion transcripts (*EML4-ALK* and *KIF5B-ALK*, respectively) were used as reported previously (the sequences of the primers used are listed in Table 1) [7,15]. The multiplex PCR conditions were 95 °C for 60 s, followed by 50 cycles of 94 °C for 15 s, 60 °C for 30 s, and 72 °C for 60 s. The PCR products were electrophoresed, and potential fusion transcripts were purified and sequenced with an ABI 3130 Sequencer using PCR primers (BigDye Terminator v3.1 Cycle Sequencing Kit, Applied Biosystems, Foster City, CA). In addition, the PCR products were subcloned into a TA-cloning vector (Invitrogen, Carlsbad, CA) and sequenced using M13 primers.

2.5. EGFR and KRAS mutation analysis

In cases 1–9, partial cDNAs of the *EGFR* (codon 700–909) and *KRAS* (codon 1–108) genes covering potential mutation hotspots were amplified by RT-PCR and sequenced as described above. The primer sequences are listed in Table 1. Case 10, for which frozen material was not available, was studied by high-resolution melting analysis for the common *EGFR* (L858R mutation and exon 19 deletion) and *KRAS* (codons 12 and 13) alterations, as performed routinely at our institution [31].

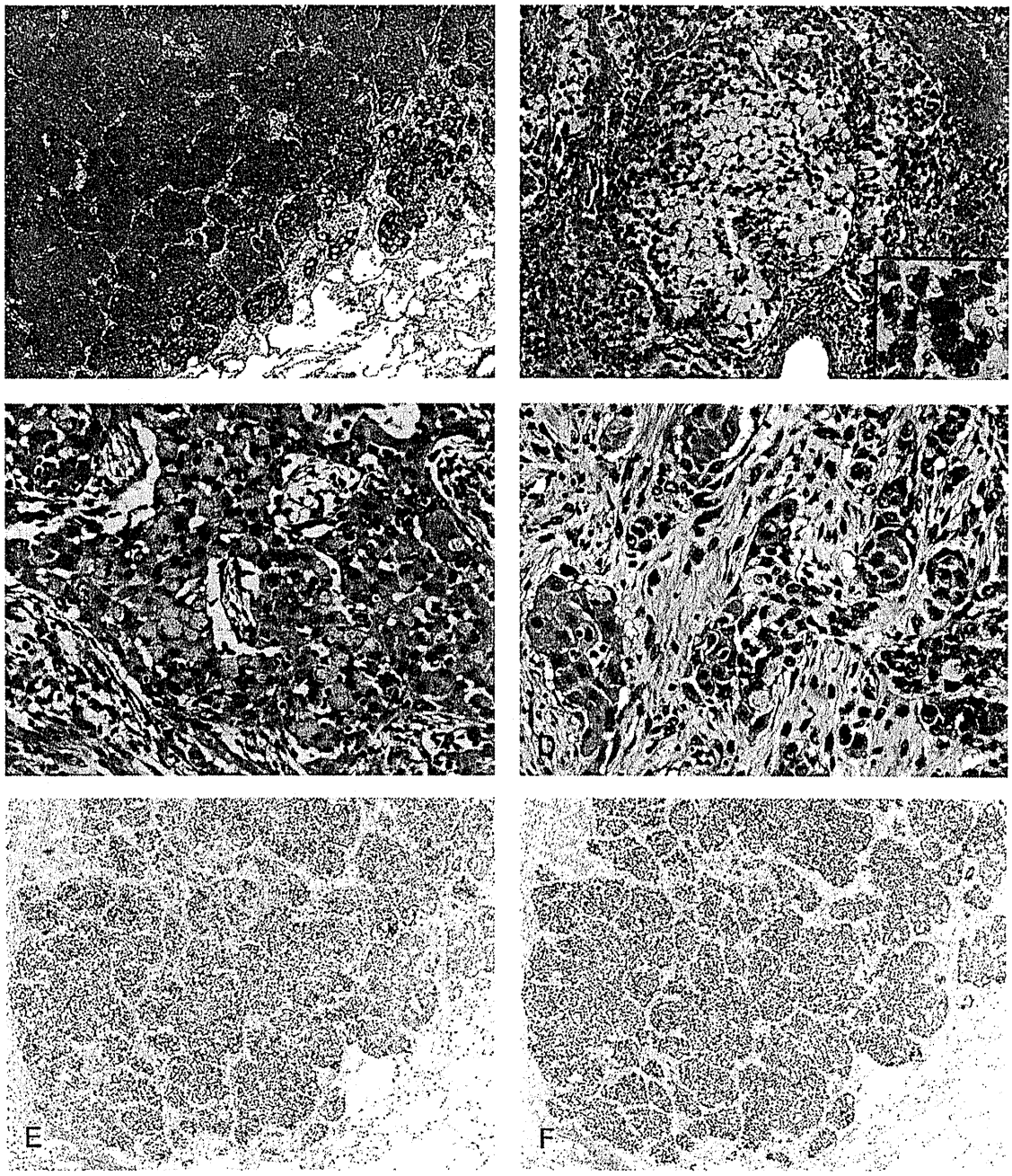

Fig. 1. Histological features of Ad-SRCCs of the lung showing solid/acinar growth with an alveolar filling pattern at the lesion periphery (A, H&E, case 1). Signet-ring cells were present at the center of a large tumor cell nest. Notice characteristic cohesive clustering of signet-ring cells and relatively monomorphic nuclei. Intracytoplasmic mucin in signet-ring cells was highlighted dark blue by alcian blue-periodic acid-Schiff (AB-PAS) staining, shown in the inset (B, H&E, case 6; inset, AB-PAS). Clusters of signet-ring cells in smaller nests (C, H&E, case 7). One tumor harboring the *EML4-ALK* fusion gene showed focal squamous differentiation (D, H&E, case 10). Fifty percent of Ad-SRCCs diffusely co-expressed TTF-1 (E, TTF-1 immunostain, case 1) and p63 (F, p63 immunostain, case 1).

3. Results

3.1. Clinicopathological features

Ten (1.4%) cases of lung Ad-SRCC were identified out of 699 consecutive primary adenocarcinomas resected at NCC Tokyo (2004–2005). The pertinent clinicopathological data are summarized in Table 2, along with the immunohistochemical and genetic results. The patients were five men and five women with a mean age of 58 (range, 33–78) years. They were slightly younger than 699 primary lung adenocarcinoma patients treated during the study period (mean age 63.4 years old, $p = 0.038$). There were five non-smokers, two light smokers (<20 pack-years), and three heavy smokers (≥20 pack-years). The tumors all appeared well circumscribed on gross examination and measured 2.7 cm in diameter on average (range, 1.0–5.0 cm). Five tumors were found at stage I, one was at stage II, and three were at stage III. Histologically, all the tumors contained, by definition, at least 5% signet-ring cells. AB-PAS staining highlighted mucin as dark blue spherules in all cases (Fig. 1B, inset). The ratio of signet-ring cells relative to the total tumor cells varied with an average of 13% (range, 5–30%). In all cases, the signet-ring cells formed tight or loose cohesive

Table 2
Clinicopathological findings, and *EGFR*, *KRAS*, and *ALK* status of the present 10 Ad-SRCCs of the lung.

Case #	Age	Sex	SI	Size (cm)	Stage	Follow-up, months	WHO predominant pattern	SRC%	Nuclear grade	TTF-1 IHC	p63 IHC	*ALK* RT-PCR	*ALK* FISH	ALK IHC	*EGFR*	*KRAS*
1	34	F	14	1.8	IA	NED, 60	Solid	20	Low	3+	3+	+	+[a]	+	WT	WT
2	60	M	29	1.8	IA	NED, 64	Acinar	5	Low	3+	3+	–	NA	–	WT	WT
3	56	F	0	4.5	IIIA	DOD, 32	Solid	5	Low	3+	1+	–	–	–	WT	WT
4	63	M	30	5.0	IIIA	AWD, 3	Acinar	5	Intermediate	3+	1+	–	Ind	–	WT	WT
5	78	M	10	3.0	IA	AWD, 53	Solid	5	Intermediate	0	0	–	–	–	WT	WT
6	63	F	0	3.0	IIIB	NED, 50	Solid	20	Low	3+	3+	–	–	–	WT	WT
7	68	M	30	2.5	IIA	NED, 51	Solid	5	Intermediate	2+	2+	–	+	–	WT	WT
8	77	F	0	2.5	IA	NED, 48	Papillary	15	Low	3+	2+	+	Ind	+	WT	WT
9	51	M	0	1.0	IIIA	NED, 47	Solid	20	Low	3+	3+	+	+	+	WT	WT
10	33	F	0	1.4	IB	NED, 62	Solid	30	Intermediate	3+	3+	NA	+[a]	+	WT	WT

F, female; M, male; SI, smoking index (number of packs of cigarettes per day × years); NED, no evidence of disease; DOD, died of disease; AWD, alive with disease; SRC%, percentage of signet-ring cells; NA, not available; Ind, indeterminate; WT, wild type.
[a] Cases showing a single orange signal and one fused signal on FISH.

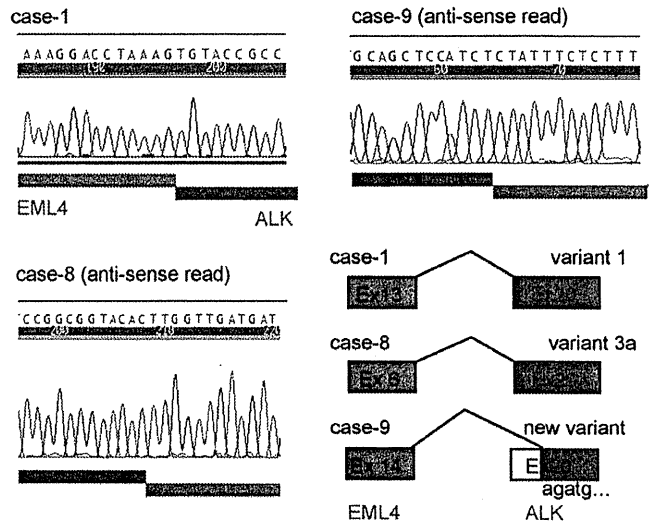

Fig. 2. RT-PCR and sequence analysis identified the presence of *EML4-ALK* fusion transcripts in three cases (cases 1, 8, and 9) of Ad-SRCC.

clusters within solid nests of tumor cells (Fig. 1B and C), typically appearing in the central portion of nests. The tumor cell nests filled and expanded the alveolar spaces at the lesional periphery in nine cases (Fig. 1A). The tumor cell nuclei were relatively monomorphic, except for focal areas of pleomorphism in case 4, and showed low- (six cases) to intermediate-grade (four cases) atypism. The predominant WHO growth pattern was solid in seven cases, acinar in two, and papillary in one. Signet-ring cells were associated with a solid pattern in eight cases, an acinar pattern in one, and both acinar and solid patterns in one. Lepidic growth was absent in all the cases except for case 6. One tumor (case 10) showed focal squamous differentiation (Fig. 1D). Extracellular mucin was minimal in all cases. Nine Ad-SRCCs were diffusely immunopositive for TTF-1 (Fig. 1E). Nine tumors were also immunoreactive for p63, and five of them showed diffuse (>50%) labeling with strong intensity (Fig. 1F). In seven cases, the foci of signet-ring cells within the tumor co-expressed TTF-1 and p63 (cases 1, 2, 6–10). Follow-up information was available for all of the patients. Seven patients were alive and well without recurrence after a mean follow-up period of 55 months (range, 47–64 months), two patients were alive with distant recurrence at 3 and 53 months, respectively. The remaining patient died of the disease 32 months after surgery.

3.2. *ALK* analysis (RT-PCR, FISH, and IHC)

The expected PCR products of the *EML4-ALK* fusion gene were observed in three out of nine tested cases, and none of the *KIF5B-ALK* fusion transcripts was amplified. The sequence of each PCR product revealed that these three cases had different fusion transcripts (Fig. 2). The detected transcripts were variant 1 in case 1 and variant 3a in case 8. Case 9 harbored a new breakpoint connecting *EML4* exon 14 and the 12-amino-acids-deleted *ALK* exon 20.

Among the three RT-PCR-proven ALK-translocated cases, unanimous agreement on the positive *ALK* rearrangement was obtained for two tumors by FISH (Fig. 3). The remaining case (case 8) was designated as indeterminate for *ALK* rearrangement, and it showed more than 2 pairs of signals in the vast majority of the tumor cells, the significance of which finding was unclear. Among the six PCR-negative cases, FISH was unsuccessful in one case, three were designated as negative, one was designated as indeterminate, and one was designated as positive for *ALK* rearrangement. The latter case (case 7) showed a small number of tumor cells exhibiting wider split signals than expected for *EML4-ALK* fusion. Case 10, whose

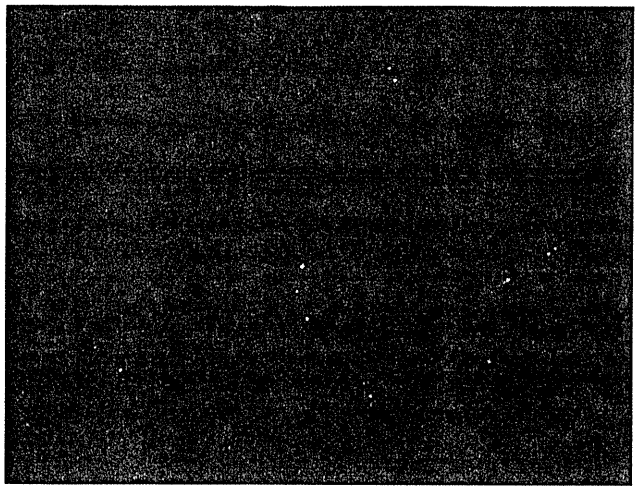

Fig. 3. FISH study using an *ALK* break-apart probe showed *ALK* rearrangement (splitting of green and orange signals) in an Ad-SRCC (case 9).

fresh tissue was not available for RT-PCR analysis, was shown to be positive for *ALK* rearrangement by FISH. In cases 1 and 10, more than 50% of the counted 100 tumor cells demonstrated loss of 5′ locus of split-apart *ALK*, showing one fused signal and one orange signal per cell.

The results of IHC were in accordance with those of PCR. All of the three PCR-positive tumors were strongly reactive for ALK antibody (Fig. 4), and all of the six PCR-negative tumors were non-reactive for this marker. Case 10, in which *ALK* rearrangement was detected by FISH, also showed strong labeling for ALK antibody.

3.3. *EGFR and KRAS mutation analyses*

No mutation of the *EGFR* or *KRAS* gene was detected by sequencing in the nine studied cases. Case 10 was also negative for *EGFR* or *KRAS* mutation by high-resolution mutation analysis.

4. Discussion

The clinical and histological findings in the present series were generally in accord with prior reports. The incidence of Ad-SRCCs in this series was 1.4%, in keeping with the rarity (0.14–1.9%) reported by other authors [21–23,26]. Younger age at onset and light tobacco exposure in the present series also concurred with the findings of other studies [21–24,32]. Unlike others [22,23,27], however, the majority of the tumors in this series had a lower stage (I or II) at presentation, and their prognoses were accordingly fair, but these findings likely reflect that all of our cases were surgically resected at the institution which treats many small-sized lung tumors. Besides their defining cytological attribute, Ad-SRCCs showed characteristic architectural profiles as described previously [21,24,27], including solid nests, cohesive clustering of signet-ring cells, and alveolar filling patterns at the lesional periphery [21,23,33]. The cohesiveness of signet-ring cells is somewhat at variance with most homonymous tumors in the stomach or breast, which often infiltrate diffusely as isolated cells. The nuclei of the Ad-SRCCs in this series were uniform and of low to intermediate grade without frank anaplasia in most cases, though the nuclear features of Ad-SRCCs have not been fully analyzed in the past [23].

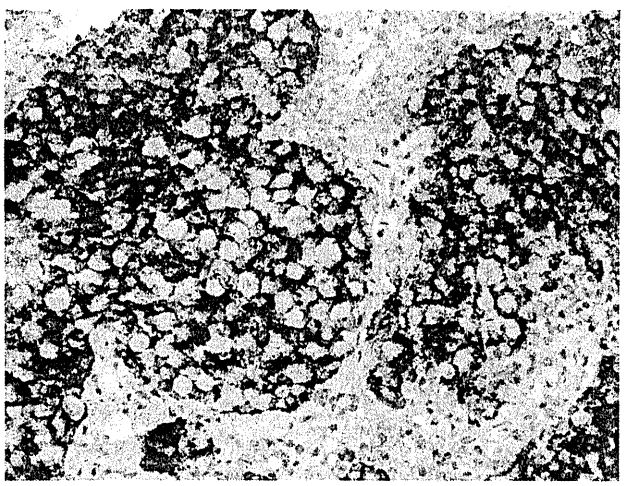

Fig. 4. ALK protein is immunohistochemically positive in an Ad-SRCC (ALK immunostain, case 1).

Immunohistochemically, most of our Ad-SRCCs were positive for TTF-1, as expected [23,26]. Interestingly, most tumors also labeled for p63, and half were stained in diffuse strong manner by this antibody. The immunoreactivity of p63 in lung adenocarcinomas is considered to be uncommon [34,35], and a recent report in abstract form [36] showed that significant co-expression of TTF-1 and p63 occurred in only 5.5% of adenocarcinomas of the lung in general. This previously unrecognized peculiar immunoprofile of Ad-SRCC may indicate that this tumor subtype might arise from a specific cell of origin, different from most lung adenocarcinomas. Although diffuse strong p63 positivity is often used as a marker of squamous cell carcinoma in diagnostic pathology, Ad-SRCC seems a major pitfall to this practice. Careful attention to the focal signet-ring cell element and TTF-1 staining should lead to the correct diagnosis.

Since ALK analysis was partly complicated by the technical difficulty of FISH (see below), we required evidence of *ALK* alteration on the basis of at least two different modalities for the diagnosis of *ALK*-translocated cancer. Four of the 10 cases (40%) of lung Ad-SRCC were thus regarded as positive for *ALK* rearrangements (cases 1, 8, 9, and 10). This result is in accord with Rodig et al. [11], who found that 14 of 47 (30%) Ad-SRCCs showed *ALK* rearrangement by FISH. *ALK*-rearranged tumors in this study had a significantly more proportion of signet-ring cell components than *ALK* wild-type tumors (mean 44% vs. 10%; $p = 0.0058$), and this trend was also in agreement with the previous report [11]. Although it was suspected that the presence of signet-ring cell in *ALK*-rearranged tumors might be a regionally/ethnically limited phenomenon [11], we showed that it is rather a universal finding also evident in non-Western patients.

Because the *EML4-ALK* fusion in lung cancer is rare (3.8%) [17] in unselected populations, and because the currently accepted methods for detecting this chimeric gene are relatively expensive and labor-intensive, a practical concentration strategy is needed for effectively preselecting a subgroup of patients whose tumors are more likely to be positive for *ALK* translocation [2]. The present study used histological criteria alone, i.e. those of Ad-SRCC, to successfully extract a subset of adenocarcinomas carrying *ALK* translocation in as many as 40% of the cases. Other clinical (e.g., younger age and minimal tobacco exposure) and histological (e.g., solid or acinar pattern) features known to be associated with *ALK*-rearranged tumors [8,12] may also be used in combination with the signet-ring cells in order to enhance the detection rate. Rodig et al. [11] indeed noted that as many as 50% of their tumors showing a combination of solid growth and the presence of >10% signet-ring cells harbored *ALK* rearrangement.

The minor discordance of *ALK* status among the modalities used in this study resulted primarily from FISH analysis, whereas the results of RT-PCR and IHC were completely concordant. Interpretation of FISH results for *EML4-ALK*-positive lung cancer is known to

be technically difficult [2,11]. Because both the *EML4* and *ALK* genes are located close to each other on the same chromosome arm, their fusion yields a split signal separated by only a short distance. Consequently, identifying a split is not as straightforward as in other translocation-associated tumors, and the criteria for recognition of positive split signals may vary among observers. Such variability may well have contributed to the present FISH results, for which opinions on two cases conflicted among different observers. One case (case 7) was interpreted as FISH-positive, as opposed to the results of RT-PCR and IHC. That tumor contained a small number of cells with *ALK*-split signals showing a much wider distance than would be expected for *EML4-ALK* fusion. The RT-PCR study of the kinase domain of *ALK* in this case showed no expression of the *ALK* gene, virtually ruling out any unknown functional translocation involving *ALK* (data not shown), and the significance of this FISH result is unclear. Although some previous studies using FISH assay with commercially available probes appeared to yield results that were more concordant with RT-PCR or IHC [6,11], our data call attention to the inherent difficulty attached to this modality, and emphasize the need for caution when integrating FISH into routine diagnostics for *ALK*-rearranged lung cancer. The development of smaller customized probes may be helpful for more reliable detection of this genetic change.

The *EML4-ALK* fusion gene detected in patient 9 in the present series is a novel variant, in which *EML4* exon 14 was joined with part of exon 20 at a point 36 nucleotides distal to the beginning of exon 20 of *ALK*. This transcript would be read in-frame to generate an intact chimeric protein that maintains the kinase domain of the *ALK* gene, and would be expected to result in overactivation of the signaling pathway downstream to ALK. The literature regarding the nomenclature of the *EML4-ALK* variants is somewhat confusing; seven variants (1, 2, 3a, 3b, 4, 5a, 5b, 6, and 7) were discovered by the same group of investigators, while two different groups have independently identified variants "4" and "5", respectively [2]. Recently, two more variants were added [14], and thus, to our knowledge, the current variant is the 12th. There are no conclusive data to indicate whether different variants are associated with different clinical or histological features.

One of the tumors shown to be positive for ALK alteration by FISH and IHC exhibited focal squamous differentiation. Although most of the previous reports have documented the exclusive adenocarcinoma histology of *ALK*-rearranged tumors, a small number have been reported to show squamous differentiation [5,6,11,16]. The current additional case further reinforces the view that the presence of *EML4-ALK* fusion is not restricted to a pure adenocarcinoma histology. Wong et al. [16] have even identified an *EML4-ALK* fusion gene in a tumor that was interpreted as mucoepidermoid carcinoma. Notably, the combination of solid growth, uniform lower-grade nuclei, clusters of mucin-rich cells, frequent diffuse p63 immunoreactivity, and rare unequivocal squamous differentiation seen in our present series of Ad-SRCCs imparted a superficial resemblance to mucoepidermoid carcinoma. However, a coexisting typical acinar or papillary growth pattern of adenocarcinoma, lack of endobronchial growth, and TTF-1 immunopositivity readily ruled out that possibility. *CRTC1-MAML2* or *CRTC3-MAML2* translocations associated with mucoepidermoid carcinomas [37] were not identified by RT-PCR in any of the present Ad-SRCCs (cases 1–9) (data not shown).

ALK-translocation-positive Ad-SRCCs in this series lacked mutations of either *EGFR* or *KRAS*, confirming the prior observations that *ALK* alteration is mutually exclusive of such genetic events [5,8,9,12,13,16]. What is particularly interesting here is that there was also a total absence of *EGFR* and *KRAS* mutations in the Ad-SRCCs without *ALK* translocations. Considering the high frequency (up to 71% [32]) of *EGFR* or *KRAS* mutations of lung adenocarcinomas in the Japanese population, our findings appear to suggest the unique genetic background of Ad-SRCC of the lung, despite the admittedly small number of cases studied. It is possible that a certain pathway downstream to the EML4-ALK chimeric protein plays a critical role in creation of the signet-ring cell morphology, and the same pathway may function even in Ad-SRCCs without *ALK* fusion genes. Alternatively, Ad-SRCCs may originate from a certain type of cell that is programmed to differentiate to a signet-ring cell phenotype, and such cells may be somehow more prone to accumulate *ALK* alterations than *EGFR* or *KRAS* mutations. It is unlikely that *EML4-ALK* itself determines the signet-ring cell cytology, because not all of the *ALK*-translocation-positive adenocarcinomas of the lung showed this particular cell type [11]. It is noteworthy that certain clinical features (younger age at onset and minimal tobacco exposure) are shared by both Ad-SRCCs and *ALK*-rearranged tumors [8,12,21,22], possibly suggesting an inherent close relationship between the two. A few previous reports have detected *KRAS* mutations in some Ad-SRCCs [24,26], and this discrepancy may be due to the small number of cases examined, or differences in the criteria used to select the Ad-SRCCs.

In conclusion, this study has confirmed the previously observed association between Ad-SRCC and *ALK*-rearrangement. The characteristic histology, immunoprofile (TTF-1/p63 co-expression), frequent *ALK* translocation, and total lack of *EGFR* or *KRAS* mutations, may suggest that Ad-SRCC forms a coherent subgroup of lung adenocarcinomas.

Conflict of interest

None declared.

Acknowledgements

The authors thank Drs. H. Mano and M. Soda for providing us information about the sequence of primers and multiplex PCR condition. We also thank Ms. Karin Yokozawa, Mr. Susumu Wakai, Ms. Sachiko Miura, and Ms. Chizu Kina for superb technical assistance. This work was supported in part by Grant-in-Aid for Cancer Research from the Ministry of Health, Labor and Welfare of Japan (T.S.), and by Grant-in-Aid for the Third-Term Comprehensive 10-Year Strategy for Cancer Control from the Ministry of Health, Labor and Welfare of Japan (H.T.).

References

[1] Travis WD, Brambilla E, Muller-Hermelink HK, Harris CC. Pathology and genetics: tumours of the lung, pleura, thymus and heart. Lyon, France: IARC Press; 2004.
[2] Horn L, Pao W. EML4-ALK: honing in on a new target in non-small-cell lung cancer. J Clin Oncol 2009;27:4232–5.
[3] Lynch TJ, Bell DW, Sordella R, Gurubhagavatula S, Okimoto RA, Brannigan BW, et al. Activating mutations in the epidermal growth factor receptor underlying responsiveness of non-small-cell lung cancer to gefitinib. N Engl J Med 2004;350:2129–39.
[4] Paez JG, Janne PA, Lee JC, Tracy S, Greulich H, Gabriel S, et al. EGFR mutations in lung cancer: correlation with clinical response to gefitinib therapy. Science 2004;304:1497–500.
[5] Soda M, Choi YL, Enomoto M, Takada S, Yamashita Y, Ishikawa S, et al. Identification of the transforming EML4-ALK fusion gene in non-small-cell lung cancer. Nature 2007;448:561–6.
[6] Boland JM, Erdogan S, Vasmatzis G, Yang P, Tillmans LS, Erickson Johnson MR, et al. Anaplastic lymphoma kinase immunoreactivity correlates with ALK gene rearrangement and transcriptional up-regulation in non-small cell lung carcinomas. Hum Pathol 2009;40:1152–8.
[7] Choi YL, Takeuchi K, Soda M, Inamura K, Togashi Y, Hatano S, et al. Identification of novel isoforms of the EML4-ALK transforming gene in non-small cell lung cancer. Cancer Res 2008;68:4971–6.
[8] Inamura K, Takeuchi K, Togashi Y, Hatano S, Ninomiya H, Motoi N, et al. EML4-ALK lung cancers are characterized by rare other mutations, a TTF-1 cell lineage, an acinar histology, and young onset. Mod Pathol 2009;22:508–15.
[9] Inamura K, Takeuchi K, Togashi Y, Nomura K, Ninomiya H, Okui M, et al. EML4-ALK fusion is linked to histological characteristics in a subset of lung cancers. J Thorac Oncol 2008;3:13–7.

[10] Koivunen JP, Mermel C, Zejnullahu K, Murphy C, Lifshits E, Holmes AJ, et al. EML4-ALK fusion gene and efficacy of an ALK kinase inhibitor in lung cancer. Clin Cancer Res 2008;14:4275–83.
[11] Rodig SJ, Mino-Kenudson M, Dacic S, Yeap BY, Shaw A, Barletta JA, et al. Unique clinicopathologic features characterize ALK-rearranged lung adenocarcinoma in the western population. Clin Cancer Res 2009;15:5216–23.
[12] Shaw AT, Yeap BY, Mino-Kenudson M, Digumarthy SR, Costa DB, Heist RS, et al. Clinical features and outcome of patients with non-small-cell lung cancer who harbor EML4-ALK. J Clin Oncol 2009;27:4247–53.
[13] Shinmura K, Kageyama S, Tao H, Bunai T, Suzuki M, Kamo T, et al. EML4-ALK fusion transcripts, but no NPM-, TPM3-, CLTC-, ATIC-, or TFG-ALK fusion transcripts, in non-small cell lung carcinomas. Lung Cancer 2008;61:163–9.
[14] Takahashi T, Sonobe M, Kobayashi M, Yoshizawa A, Menju T, Nakayama E, et al. Clinicopathologic features of non-small-cell lung cancer with EML4-ALK fusion gene. Ann Surg Oncol 2010;17:889–97.
[15] Takeuchi K, Choi YL, Togashi Y, Soda M, Hatano S, Inamura K, et al. KIF5B-ALK, a novel fusion oncokinase identified by an immunohistochemistry-based diagnostic system for ALK-positive lung cancer. Clin Cancer Res 2009;15:3143–9.
[16] Wong DW, Leung EL, So KK, Tam IY, Sihoe AD, Cheng L, et al. The EML4-ALK fusion gene is involved in various histologic types of lung cancers from nonsmokers with wild-type EGFR and KRAS. Cancer 2009;115:1723–33.
[17] Solomon B, Varella-Garcia M, Camidge DR. ALK gene rearrangements: a new therapeutic target in a molecularly defined subset of non-small cell lung cancer. J Thorac Oncol 2009;4:1450–4.
[18] Soda M, Takada S, Takeuchi K, Choi YL, Enomoto M, Ueno T, et al. A mouse model for EML4-ALK-positive lung cancer. Proc Natl Acad Sci USA 2008;105:19893–7.
[19] Kwak EL, Camidge DR. Clinical activity observed in a phase I dose escalation trial of an oral c-met and ALK inhibitor, PF-02341966. J Clin Oncol 2009:27.
[20] Kish JK, Ro JY, Ayala AG, McMurtrey MJ. Primary mucinous adenocarcinoma of the lung with signet-ring cells: a histochemical comparison with signet-ring cell carcinomas of other sites. Hum Pathol 1989;20:1097–102.
[21] Tsuta K, Ishii G, Yoh K, Nitadori J, Hasebe T, Nishiwaki Y, et al. Primary lung carcinoma with signet-ring cell carcinoma components: clinicopathological analysis of 39 cases. Am J Surg Pathol 2004;28:868–74.
[22] Ou SH, Ziogas A, Zell JA. Primary signet-ring carcinoma (SRC) of the lung: a population-based epidemiologic study of 262 cases with comparison to adenocarcinoma of the lung. J Thorac Oncol 2010;5:420–7.
[23] Castro CY, Moran CA, Flieder DG, Suster S. Primary signet ring cell adenocarcinomas of the lung: a clinicopathological study of 15 cases. Histopathology 2001;39:397–401.
[24] Hayashi H, Kitamura H, Nakatani Y, Inayama Y, Ito T, Kitamura H. Primary signet-ring cell carcinoma of the lung: histochemical and immunohistochemical characterization. Hum Pathol 1999;30:378–83.
[25] Merchant SH, Amin MB, Tamboli P, Ro J, Ordonez NG, Ayala AG, et al. Primary signet-ring cell carcinoma of lung: immunohistochemical study and comparison with non-pulmonary signet-ring cell carcinomas. Am J Surg Pathol 2001;25:1515–9.
[26] Maeshima A, Miyagi A, Hirai T, Nakajima T. Mucin-producing adenocarcinoma of the lung, with special reference to goblet cell type adenocarcinoma: immunohistochemical observation and Ki-ras gene mutation. Pathol Int 1997;47:454–60.
[27] Iwasaki T, Ohta M, Lefor AT, Kawahara K. Signet-ring cell carcinoma component in primary lung adenocarcinoma: potential prognostic factor. Histopathology 2008;52:639–40.
[28] Tsuta K, Ishii G, Nitadori J, Murata Y, Kodama T, Nagai K, et al. Comparison of the immunophenotypes of signet-ring cell carcinoma, solid adenocarcinoma with mucin production, and mucinous bronchioloalveolar carcinoma of the lung characterized by the presence of cytoplasmic mucin. J Pathol 2006;209:78–87.
[29] Sobin LH, Wittekind C, editors. International Union Against Cancer (UICC) TNM classification of malignant tumours. 6th ed. New York: Wiley-Liss; 2002.
[30] Paik J, Choe J, Chung J. Protein expression and gene rearrangement of ALK in non-small cell lung carcinomas. Mod Pathol 2010;23:411A.
[31] Fukui T, Ohe Y, Tsuta K, Furuta K, Sakamoto H, Takano T, et al. Prospective study of the accuracy of EGFR mutational analysis by high-resolution melting analysis in small samples obtained from patients with non-small cell lung cancer. Clin Cancer Res 2008;14:4751–7.
[32] Sakuma Y, Matsukuma S, Yoshihara M, Nakamura Y, Noda K, Nakayama H, et al. Distinctive evaluation of nonmucinous and mucinous subtypes of bronchioloalveolar carcinomas in EGFR and K-ras gene-mutation analyses for Japanese lung adenocarcinomas: confirmation of the correlations with histologic subtypes and gene mutations. Am J Clin Pathol 2007;128:100–8.
[33] Sarma DP, Hoffmann EO. Primary signet-ring cell carcinoma of the lung. Hum Pathol 1990;21:459–60.
[34] Sheikh HA, Fuhrer K, Cieply K, Yousem S. p63 expression in assessment of bronchioloalveolar proliferation of the lung. Mod Pathol 2004;17:1134–40.
[35] Wu M, Orta L, Gil J, Li G, Hu A, Burstein DE. Immunohistochemical detection of XIAP and p63 in adenomatous hyperplasia, atypical adenomatous hyperplasia, bronchioloalveolar carcinoma and well-differentiated adenocarcinoma. Mod Pathol 2008;21:553–8.
[36] Ang D, Ghaffar H, Zakowski M, Teruya-Feldstein J, Moreira A, Rekhtman N. Expression of squamous markers in lung adenocarcinoma: clinicopathologic and molecular correlates, and implications for differentiation from squamous cell carcinoma. Mod Pathol 2010;23:397A.
[37] Nakayama T, Miyabe S, Okabe M, Sakuma H, Ijichi K, Hasegawa Y, et al. Clinicopathological significance of the CRTC3-MAML2 fusion transcript in mucoepidermoid carcinoma. Mod Pathol 2009;22:1575–81.

Japanese Society of Thoracic Radiology

A Case of Malignant Pleural Mesothelioma With Osseous and Cartilaginous Differentiation

Natsuko Shiba, MD, Masahiko Kusumoto, MD,* Koji Tsuta, MD,† Hirokazu Watanabe, MD,* Shun-ichi Watanabe, MD,‡ Naobumi Tochigi, MD,† and Yasuaki Arai, MD**

Abstract: A 69-year-old man with a history of exposure to asbestos was admitted because of a chest radiographic abnormality. Subsequent findings from computed tomography and a thoracoscopic biopsy suggested malignant mesothelioma. Punctate calcification was observed in the pleural tumor on computed tomography scanning. The patient underwent pleuropneumonectomy, and the tumor was pathologically diagnosed as malignant mesothelioma, sarcomatoid type with osseous and cartilaginous differentiation. Malignant mesothelioma with osseous and cartilaginous differentiation is a rare condition. Punctate calcification in the pleural mass as a lesion distinct from the pleural plaque may indicate osseous or osteosarcomatous differentiation in malignant mesothelioma.

Key Words: malignant pleural mesothelioma, osseous differentiation, cartilaginous differentiation, computed tomography, calcification

(*J Thorac Imaging* 2011;26:W30–W32)

Malignant pleural mesothelioma is a rare primary tumor of the pleura. It is macroscopically classified as localized or diffuse type, and histologically divided into epithelioid, sarcomatoid, desmoplastic, and biphasic types according to the World Health Organization Classification of Tumours, 2004.[1]

Osseous and/or cartilaginous differentiation is an extremely rare presentation in malignant mesothelioma. Osteosarcomatous lesions that appear as dense, punctate calcified foci on computed tomography (CT) scans are rarer still, and only a few cases have been reported.[2–5] Here, we report a case of malignant pleural mesothelioma with osseous and cartilaginous differentiation, in which dense, punctate calcifications were observed on CT scanning.

CASE REPORT

A 69-year-old man who had no significant past medical history was admitted to the department of thoracic surgery. Five months before admission, the patient was asymptomatic but had an abnormal chest radiograph. Results from a subsequent CT scan and thoracoscopic biopsy suggested the diagnosis of malignant mesothelioma. The patient was a building contractor and had been exposed to asbestos for 48 years. There were no significant findings on physical examination. Findings from laboratory tests and tumor markers, including carcinoembryonic antigen, cytokeratin fragment, cancer antigen 19-9, and pro-gastrin-releasing peptide, were within normal range; however, levels of neuron-specific enolase and squamous cell carcinoma antigen were slightly elevated.

Chest x-ray revealed an approximately 10-cm mass with clear margins in the right middle hemithorax and a smaller caudal mass (Fig. 1). In addition, right-sided pleural thickening was observed. CT scanning revealed masses contiguous with the right pleura, and dense, calcified foci were detected in the main tumor (Fig. 2). The calcifications were punctate and uniform (largest diameter, 5 mm) and were diffusely scattered throughout the tumor. Linear calcification also appeared in the pleural plaque. In the lung window setting, the right lung parenchyma was compressed by the pleural tumors, but no tumors were observed within the right lung parenchyma or the left hemithorax. There was no evidence of pulmonary fibrosis.

Right pleuropneumonectomy was performed with chest wall resection. Macroscopic examination revealed multiple nodules and tumors, which arose from the parietal pleura. The largest tumor, which was yellowish white and 9 cm in diameter with clear margins, compressed the right lung adjacent to the tumor (Fig. 3A). Calcifications could be palpated in the tumor and pleura.

Histologic examination revealed a solid growth pattern with oval-to-elongated spindle cells (Fig. 3B). Osteosarcomatous components were scattered in the tumor nests (Fig. 3C), and focal chondrosarcomatous components were observed. Although the tumor invaded the lung parenchyma, most of the tumor grew in the parietal and visceral pleurae. Immunohistochemical examination revealed atypical spindle cells that expressed positive mesothelioma

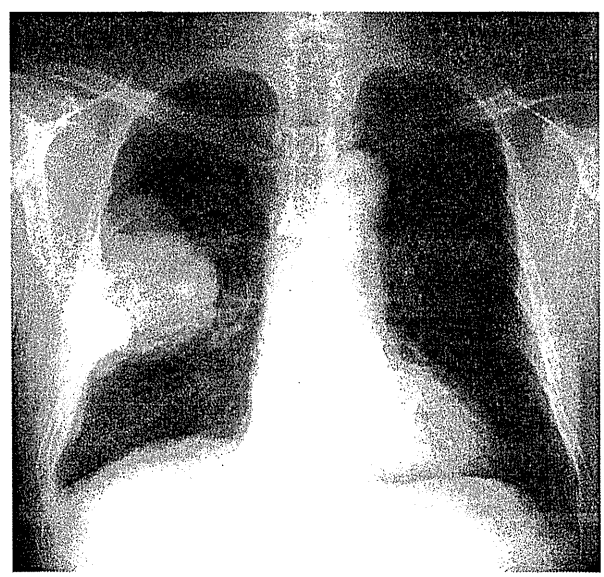

FIGURE 1. Chest radiograph showing well-defined tumor masses in the right hemithorax.

From the *Divisions of Diagnostic Radiology; †Clinical Laboratory; and ‡Thoracic Surgery, National Cancer Center Hospital, Tokyo, Japan.

Reprints: Masahiko Kusumoto, MD, Division of Diagnostic Radiology, National Cancer Center Hospital, 5-1-1 Tsukiji, Chuo-ku, Tokyo, 104-0045, Japan (e-mail: mkusumot@ncc.go.jp).

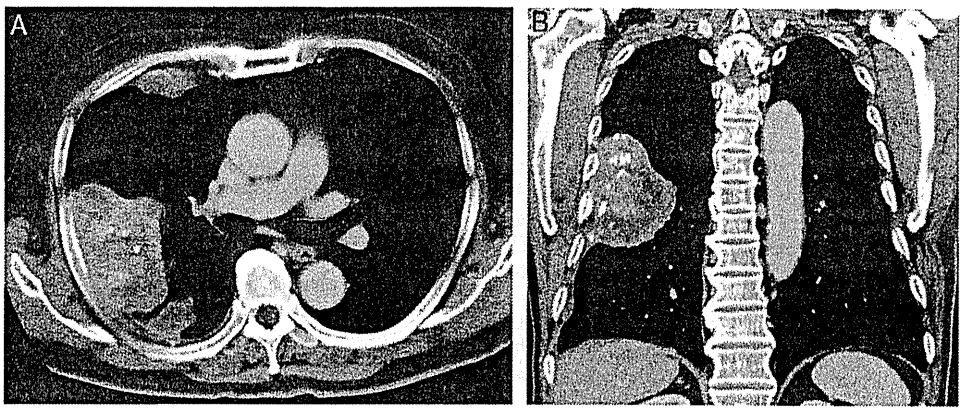

FIGURE 2. A, Axial contrast-enhanced CT scan of the thorax showing masses in the right pleura. Punctate calcifications were detected in the main tumor. B, Coronal reformatted image clearly shows that the tumor arises from the pleura.

markers (calretinin, podoplanin, and Wilms tumor-1), but did not express negative mesothelioma markers (carcinoembryonic antigen, thyroid transcription factor-1, and Ber-Ep4). Asbestos bodies were detected in the lung parenchyma. On the basis of these findings, we diagnosed malignant pleural sarcomatoid mesothelioma with osseous and cartilaginous differentiation.

The patient developed both local recurrence and metastasis and died 19 months after surgery.

DISCUSSION

Malignant pleural mesothelioma is a rarely encountered, high-grade malignant primary tumor. Cases among men have declined in the United States[6]; however, the incidence is increasing in Japan.[7] Development of osseous or cartilaginous differentiation in malignant mesothelioma is very rare, and Goldstein first reported 2 cases in 1979.[8] He suggested that the pluripotentiality of coelomic mesothelium may be the cause of its differentiation toward bone and cartilage, and also proposed the following alternative hypotheses: (1) the cartilage and bone, developed separately from the neoplasm, could be caused by previous tuberculous pleurisy; (2) the mesothelioma might have produced a substance that promoted cartilage and bone formation, directly or by stimulating the parathyroid glands; (3) the cartilage and bone might be integral components of the neoplasm and in parts the spindle cells might be merging or transforming into the cartilage; (4) 2 separate neoplasms may have been present, a mesothelioma with classical tubular formation and a fibrochondrosarcoma; and (5) asbestotic pleural plaques often undergo calcification.

Bolen et al[9] demonstrated the process by which subserous connective tissue cells obtained epithelial characteristics. They suggested that the pathogenesis is caused by the multipotency of mesothelial cells, using the term multipotential subserosal cells, which supports the hypothesis of pluripotent coelomic mesothelium proposed by Goldstein.[8] Yousem and Hochholzer[10] also favored this hypothesis. Our case supports this hypothesis, as there was no evidence of tuberculosis infection or other primary

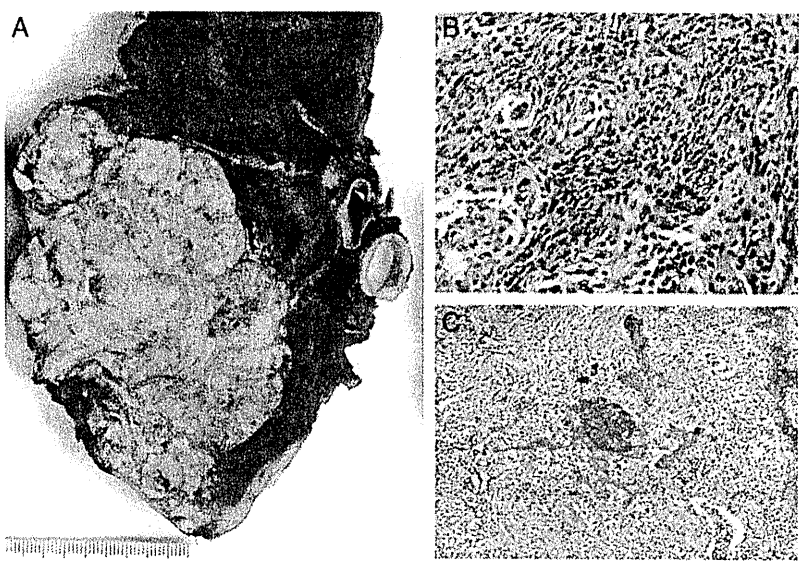

FIGURE 3. A, The cut surface of the largest tumor. The tumor has a diameter of 9 cm, is composed of yellowish white nodules with focal ossification, and is compressing the right lower lobe of the lung. B, Sarcomatoid mesothelioma shows oval-to-elongated spindle cells. C, Irregular-shaped osteoid components with calcium deposition are observed in the nests.

tumors and the osseous lesion was not colocalized with asbestos plaque. However, the possibility of parathyroid hormone influence cannot be excluded.

Of the 2 cases reported by Goldstein,[8] one case showed osteosarcomatous differentiation, and the other showed bone and cartilage differentiation. Sonja et al[11] summarized 27 cases of malignant mesothelioma with heterologous elements. In their report, they suggested that the term "heterologous" should be reserved for tumors that show malignant heterologous elements, such as osteosarcomatous, chondrosarcomatous, or rhabdomyoblastic elements. Pathologically, the differential diagnosis of these cases includes a primary or secondary pleural sarcoma. They concluded that mesothelioma cannot be excluded if cytokeratin staining is negative and should be diagnosed by anatomic distribution. The prognosis after diagnosis of mesothelioma with heterologous elements is similar to that associated with pleural mesothelioma of the sarcomatoid type; survival is approximately 6 months. Our case included heterologous elements such as osteosarcomatous and chondrosarcomatous differentiation.

Several reports have described imaging findings of pleural mesothelioma, but only 3 reports mentioned tumor calcifications detected by CT scanning.[2–5] Arnold et al[2] reported 2 cases of diffuse malignant mesothelioma that presented with large and dense calcified pleural masses, which were visualized on CT scan. In this report, it was described that the diagnosis of osteocartilaginous differentiation in diffuse malignant mesothelioma was based on the past history of asbestosis exposure, the typical radiographic appearance of encasing pleural tumor, the histopathologic features of malignant mesothelioma, and the absence of any osteogenic sarcoma or chondrosarcoma elsewhere. In this case, large calcification inside the main tumor was not seen, but punctate calcification was evident on CT scanning. Calcification of benign pleural plaque and osseous differentiation in mesothelioma could be distinguished by their shape and location. Calcification of benign pleural plaque is linear and is located on thickened pleural plaque, whereas osseous differentiation in mesothelioma is punctate or large and is located inside the tumor. The radiologic differential diagnoses of malignant pleural tumor with calcification include lung cancer with pleural dissemination, sarcoma derived from pleura, and metastatic lung or pleural tumor, such as colorectal cancer, osteosarcoma, and chondrosarcoma.

In conclusion, we report a case of malignant mesothelioma with osseous and cartilaginous differentiation. The punctate calcifications in the pleural tumor, distinct from the pleural plaque, may indicate osseous or osteosarcomatous differentiation in malignant mesothelioma.

REFERENCES

1. William D, Travis MD. *Pathology & Genetics of Tumours of the Lung, Thymus and Heart (World Health Organization Classification of Tumours)*. Lyon, France: IARC Press; 2004: 126–136.
2. Arnold R, Arnold S, William H, et al. Calcification as a sign of sarcomatous degeneration of malignant mesothelioma: a new CT finding. *J Comput Assist Tomogr*. 1996;20:42–44.
3. Okamoto T, Yokota S, Arakawa S, et al. Pleural malignant mesothelioma with osseus cartilaginous and rhabdomyogenic differentiation. *Nihon Kokyuki Gakkai Zasshi*. 1998;36:696–701. In Japanese.
4. Narita K, Iwanami H, Hiyoshi H, et al. A case of a huge malignant mesothelioma with extensive ossification resected by transverse sternotomy with bilateral thoracotomy. *Jpn J Lung Cancer*. 2001;53:661–666. In Japanese.
5. Hillerdal G, Elmberger G. Malignant mediastinal tumor with bone formation—mesothelioma or sarcoma? *J Thorac Oncol*. 2007;10:983–984.
6. Bertram P, Adam W. Mesothelioma trends in the United States: an update based on surveillance, epidemiology, and end results program data for 1973 through 2003. *Am J Epidemiol*. 2004;159:107–112.
7. Murayama T, Takahashi K, Natori Y, et al. Estimation of future mortality from pleural malignant mesothelioma in Japan based on an age-cohort model. *Am J Ind Med*. 2006; 49:1–7.
8. Goldstein B. Two malignant pleural mesotheliomas with unusual histological features. *Thorax*. 1979;34:375–379.
9. Bolen JW, Hammar SP, McNutt MA. Reactive and neoplastic serosal tissue. *Am J Surg Pathol*. 1986;10:34–47.
10. Yousem SA, Hochholzer L. Malignant mesotheliomas with osseus and cartilaginous differentiation. *Arch Pathol Lab Med*. 1987;111:62–66.
11. Sonja K, Annabelle M, Douglas WH, et al. Malignant mesothelioma with heterologous elements: clinicoparhological correlation of 27 cases and literature review. *Mod Pathol*. 2008;21:1084–1094.

Which is the Better Prognostic Factor for Resected Non-small Cell Lung Cancer

The Number of Metastatic Lymph Nodes or the Currently Used Nodal Stage Classification?

Shenhai Wei, MD, PhD,† Hisao Asamura, MD,* Riken Kawachi, MD,* Hiroyuki Sakurai, MD,* and Shun-ichi Watanabe, MD**

Introduction: This retrospective study was conducted to evaluate the prognostic significance of the number of metastatic lymph nodes (nN) in resected non-small cell lung cancer (NSCLC) in comparison with the currently used pathologic nodal (pN) category in the staging system.

Methods: A total of 1659 patients who underwent potentially curative resection for NSCLC from 2000 to 2006 were included in this study. The association between the nN and survival was explored, and the results were compared with those using the location-based pN stage classification.

Results: The patients were divided into four categories according to the number of metastatic nodes: nN0, absence of metastatic nodes; nN1, metastasis in one to two nodes; nN2, metastasis in three to six nodes; and nN3, metastasis in seven or more nodes. The 5-year overall survival for nN0, nN1, nN2, and nN3 was 89.2%, 65.1%, 42.1%, and 22.4%, respectively ($p < 0.001$). The nN category could be used to subdivide pN1 and pN2 patients into two (nN1 and nN2) and three (nN1, nN2, and nN3) prognostically distinct subgroups, respectively. Multivariate analysis showed the nN category was an independent prognostic factor for resected NSCLC. The difference in overall survival between pN1 and pN2 was not significant (55.4% versus 47.8%, $p = 0.245$). Patients in each nN category could not be subdivided into different prognostic subgroups according to the pN classification.

Conclusions: The nN category in this study was shown to be a better prognostic determinant than the location-based pN stage classification.

Key Words: Non-small cell lung cancer, Lymph node metastasis, Prognosis.

(*J Thorac Oncol.* 2011;6: 310–318)

*Division of Thoracic Surgery, National Cancer Center Hospital, Tokyo, Japan; and †Department of Thoracic Surgery, First Hospital of Tsinghua University, Beijing, China.

Disclosure: The authors declare no conflicts of interest.

Address for correspondence: Dr. Hisao Asamura, Division of Thoracic Surgery, National Cancer Center Hospital, 5-1-1, Tsukiji, Chuo-ku, Tokyo 104-0045, Japan. E-mail: hasamura@ncc.go.jp

ISSN: 1556-0864/11/0602-0310

The accurate assessment of lymph node involvement is crucial for the diagnosis and treatment of non-small cell lung cancer (NSCLC). Recently, the seventh edition of the tumor-node-metastasis (TNM) classification for NSCLC has been accepted with some modifications in comparison with the sixth edition.[1] However, the node (N) descriptor in the new classification remains the same as in the previous edition and depends solely on the anatomic extent of lymph node involvement despite the change in the nodal map.

Patients suffering from pathologic N1 or N2 disease in NSCLC have long been known to exhibit prognostic heterogeneity.[2–13] This has indicated that it is necessary to refine the currently used pathologic N (pN) stage classification and has justified attempts to identify alternative nodal classification methods. In some other solid tumors, such as breast, gastric, and colorectal cancer, the number of metastatic lymph nodes has been considered in the TNM staging system.[14] Recently, the number of metastatic lymph nodes (nN), when classified into several categories, has been shown to be a prognostic factor for resected NSCLC.[9,15] However, to date, it is still unknown whether the nN category or the pN stage classification is the better prognostic factor. In this study, we retrospectively evaluated the association between the nN category and the prognosis of resected NSCLC and compared the results with the classic pN stage classification.

PATIENTS AND METHODS

Patient Selection

A total of 2333 consecutive patients with NSCLC who underwent surgery at the National Cancer Center Hospital, Tokyo, from January 2000 to December 2006 were examined retrospectively. The Institutional Review Board approved this retrospective study, and informed consent from patients was waived.

All the patients received a thorough work-up preoperatively, including computed tomography (CT) scan, chest radiograph, blood test, and positron emission tomography (PET), if necessary, to evaluate their eligibility for surgery. Patients who were identified to have distant metastasis or clinical N2 (cN2) diseases preoperatively were excluded from

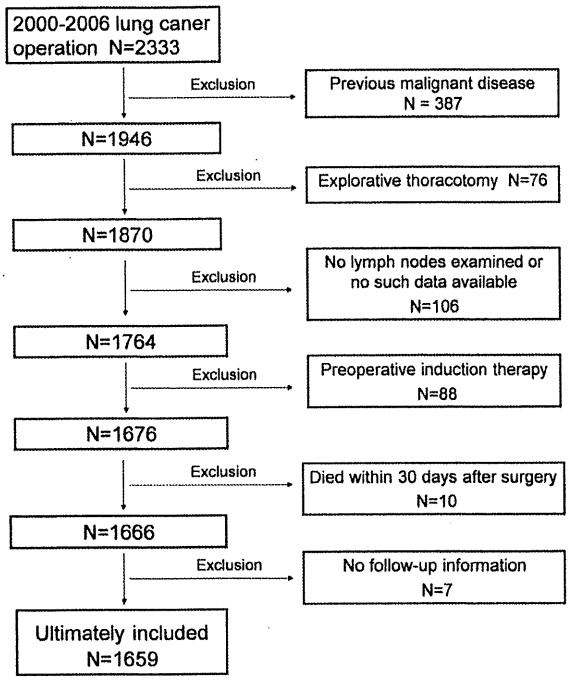

FIGURE 1. Patients included in this study.

surgery. Clinical N2 disease was suspected when mediastinal lymph node enlargement was present with a minimal diameter of 1.0 cm or more on the CT scan. If the following PET scan or mediastinoscopy was positive, we considered it as cN2 disease and excluded from surgery. PET scan and mediastinoscopy were used only for suspected cN2 disease rather than for all patients.

Patients with a prior history of malignant disease or induction therapy before surgery and those who underwent explorative thoracotomy were not included in this study. In addition, those who died within 30 days after surgery, those for whom no lymph node was retrieved or no such data were available, and those for whom follow-up information was unavailable were also excluded. Ultimately, a total of 1659 patients were included in this study (Figure 1).

Procedure Performed

Procedures performed for the affected pulmonary consisted of wedge resection/segmentectomy, lobectomy, bilobectomy, and pneumonectomy. Wedge resection or segmentectomy was performed only for the high-risk patients, combined with minimal lymph node dissection, sometimes maybe around the hilum only. For all the other patients, we performed lymph node dissection based on the lobe-specific patterns of nodal metastases.[16,17] When the cancer located in right upper lobe or left upper division, the hilar lymph nodes and upper mediastinal lymph nodes were dissected. The upper mediastinal lymph nodes indicate highest mediastinal nodes, paratracheal nodes, pretracheal nodes, and tracheobronchial nodes in right side and aortopulmonary window nodes, paraaortic nodes, and tracheobronchial nodes in left side. If intraoperative frozen section of the lymph node in either hilum or upper mediastinum was positive, we performed subcarinal dissection, which was omitted otherwise. For the tumor located in right middle lobe or left lingular segment, the lymph nodes in both upper mediastinum and subcarina were routinely dissected in addition to the hilum. When the tumor located in lower lobe, the hilar and lower mediastinal lymph nodes (including stations 7, 8, and 9) were dissected. If intraoperative pathologic examination of either the hilar or the lower mediastinal lymph node was positive, we performed additionally upper mediastinum dissection, which was omitted otherwise.

Data Collected and Statistical Analyses

The data collected included the patient demographics, surgical procedures, and pathologic reports including the histologic type, T stage, and the number and location of all the malignant and benign lymph nodes. The TNM classification was based on the sixth edition of the TNM staging system.[18]

We choose overall survival (OS) and disease-free survival (DFS) as the end points. OS was the time between surgery and death from any cause. DFS was the time from surgery to locoregional or distant relapse of lung cancer, and if without relapse, any deaths due to causes other than lung cancer would be censored. Continuous variables are expressed as the mean ± SD. The associations between variables were analyzed by either χ^2 test or Mann-Whitney and Wilcoxon tests. Survival curves were generated by the Kaplan-Meier method, and differences in survival among subgroups were examined by the log-rank test. A multivariate analysis was performed using Cox proportional hazards models to examine the association between survival and potential prognostic factors. A probability value of less than 0.05 was considered to be significant. All statistical calculations were performed using SPSS for Windows version 11.5 (SPSS Inc., Chicago, IL).

RESULTS

Patient Characteristics

The 1659 patients in this study consisted of 962 men and 697 women with a mean age of 63.8 ± 10.0 years (range, 26–89 years). The characteristics of the patients are shown in Table 1. The most frequent procedure performed was lobectomy (86.4%, n = 1434), followed by wedge resection/segmentectomy (5.4%, n = 90). Adenocarcinoma was found in 78.3% (n = 1299) of the patients, and the second most common histologic type was squamous cell carcinoma (17.4%, n = 288). A positive surgical margin was confirmed in 95 (5.7%) patients by pathologic examination. A total of 102 (6.1%) patients were classified as stage IIIb due to pleural dissemination or separate tumor nodule(s) in the same lobe identified during the operation, rather than pN3 disease. Stage IV disease (0.4%, n = 7) consisted of separate tumor nodule(s) in a different ipsilateral lobe identified during surgery.

TABLE 1. Patient Characteristics

Patient Characteristics	*N* (%)
Age (range)	63.8 ± 10.0 (26–89)
Gender	
Male	962 (58%)
Female	697 (42%)
Surgical procedure	
Wedge resection/segmentectomy	90 (5.4%)
Lobectomy	1434 (86.4%)
Bilobectomy	60 (3.6%)
Pneumonectomy	75 (4.5%)
Surgical margin	
Positive	95 (5.7%)
Negative	1564 (94.3%)
Histological type	
Adenocarcinoma	1299 (78.3%)
Squamous cell carcinoma	288 (17.4%)
Large cell carcinoma	53 (3.2%)
Adenosquamous carcinoma	19 (1.1%)
pT stage	
pT1	953 (57.4%)
pT2	500 (30.1%)
pT3	109 (6.6%)
pT4	97 (5.8%)
pN stage	
pN0	1203 (72.5%)
pN1	213 (12.8%)
pN2	243 (14.6%)
UICC stage (sixth edition)	
Ia	813 (45.0%)
Ib	302 (18.2%)
IIa	65 (3.9%)
IIb	156 (9.4%)
IIIa	214 (12.9%)
IIIb	102 (6.1%)
IV	7 (0.4%)

UICC, International Union Against Cancer.

Lymph Node Metastasis and Definition of nN Category

The mean number of lymph nodes retrieved from each patient was 15.9 ± 9.5 (range, 1–79). Lymph node metastasis was seen in 456 patients. The mean number of metastatic lymph nodes was 4.11 ± 4.43 (range, 1–29). Among the patients with nodal metastasis, 213 were identified as pN1 and 243 were pN2. The distribution of the number of metastatic lymph nodes in pN1 and pN2 is shown in Figure 2. The pN2 stage had more lymph node metastasis than pN1 (5.74 ± 5.35 versus 2.26 ± 1.71, $p < 0.001$) (Table 2).

The last follow-up visit was in August 2007, and the median follow-up duration was 30.0 months (range, 1–88 months). During the follow-up period, 386 cases suffered from locoregional or distant recurrence of lung cancer, and 214 cases died due to any cause. The 5-year OS and DFS rates for the overall population were 78.9% and 68.4%, respectively.

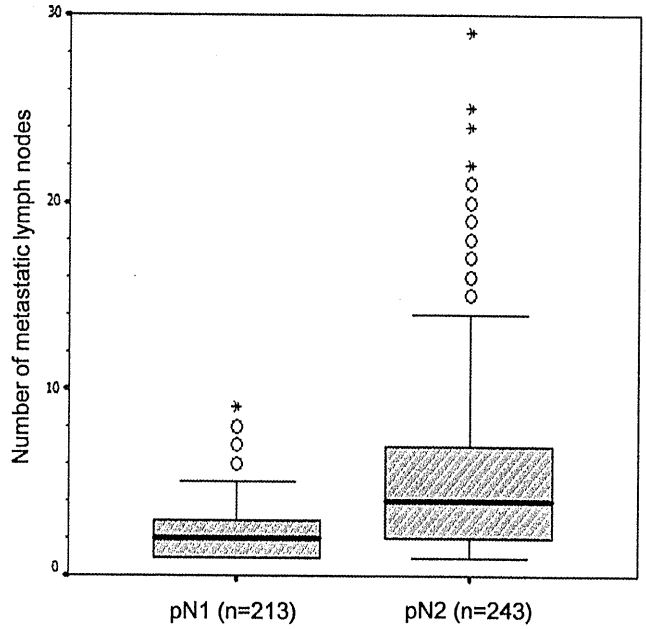

FIGURE 2. Distribution of the metastatic lymph nodes in pN1 and pN2 stage.

TABLE 2. Comparison of Number of Metastatic Lymph Nodes between pN1 and pN2 Stage

pN Stage	Number of Metastatic Lymph Nodes (Mean ± SD)	*p*
pN1	2.26 ± 1.71	<0.001
pN2	5.74 ± 5.35	

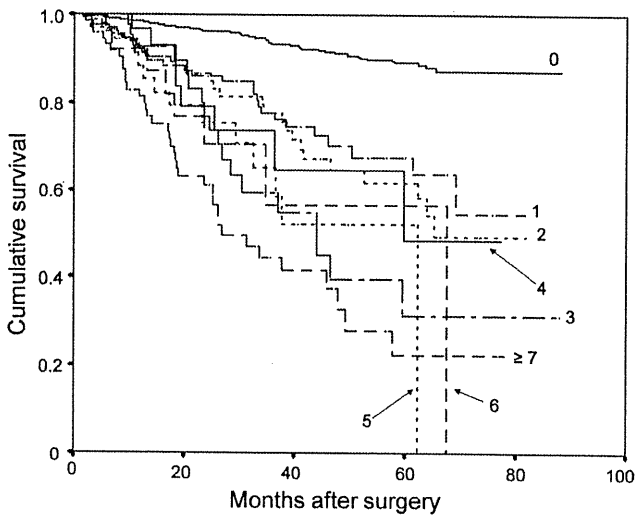

FIGURE 3. The survival curves according to different number of metastatic lymph nodes.

OS deteriorated with an increase in the number of metastatic lymph nodes (Figure 3). We classified the patients into four nN categories, and the survival curves that were

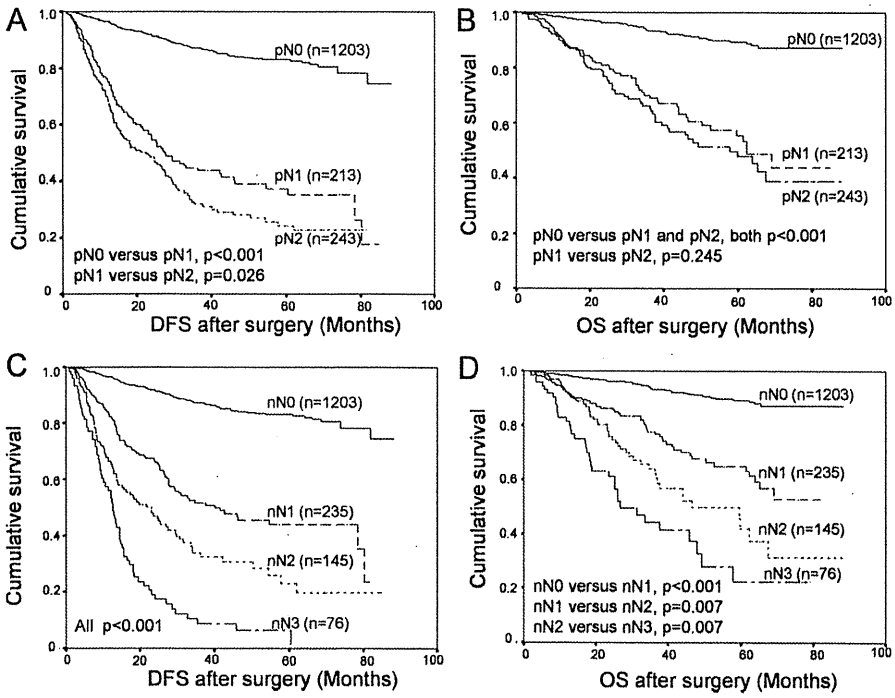

FIGURE 4. Disease-free survival (DFS) and overall survival (OS) according to pN stage classification and nN category. *A*, DFS curves according to pN stage classification. Five-year DFS rate for pN0, pN1, and pN2 was 83.2%, 37.3%, and 24.5%, respectively. *B*, OS curves according to pN stage classification. Five-year OS rate for pN0, pN1, and pN2 was 89.2%, 55.4%, and 47.8%, respectively. *C*, DFS curves according to nN category. Five-year DFS rate for nN0, nN1, nN2, and nN3 was 83.2%, 44.1%, 23.0%, and 6.5%, respectively. *D*, OS curves according to nN category. Five-year OS rate for nN0, nN1, nN2, and nN3 was 89.2%, 65.1%, 42.1% and 22.4%, respectively.

close to each other were grouped into a single category. Finally, the four nN categories were defined as follows: nN0, no lymph node metastasis; nN1, metastasis in one to two nodes; nN2, metastasis in three to six nodes; and nN3, metastasis in seven or more lymph nodes.

Prognostic Significance of nN Category and Comparison with pN Stage Classification

The OS and DFS in each pN stage classification and nN category were explored. Patients without lymph node metastasis (pN0 and nN0) had the most favorable prognosis, with 5-year OS and DFS rates of 89.2% and 83.2%, respectively. There was a significant difference between pN1 and pN2 disease with regard to DFS (5-year DFS rate: 37.3% versus 24.5%, $p = 0.026$), but the difference in OS was not significant (5-year OS rate: 55.4% versus 47.8%, $p = 0.245$) (Figures 4*A*, *B*). DFS and OS according to the nN category are shown in Figures 4*C*, *D*. The survival curves showed clear differences in OS and DFS for each of the nN categories (5-year OS rate for nN0, nN1, nN2, and nN3 was 89.2%, 65.1%, 42.1%, and 22.4%, respectively, $p < 0.001$; 5-year DFS rate was 83.2%, 44.1%, 23.0%, and 6.5%, respectively, $p < 0.001$).

A validation of the results of the nN category in terms of OS across each pT stage was performed. The results were showed in Figure 5. Although the differences between each pair of nN categories were not always significant, there was a clear tendency of deterioration of the OS from nN0 to nN3 subgroup, and the curves were apart from each other in pT1 and pT2 patients. There were similar results in terms of DFS (data not shown).

When pN1 patients were subdivided into nN1, nN2, and nN3 subgroups, there was a significant difference between the nN1 and nN2 subgroups with regard to both OS (5-year OS rate: 61.5% versus 35.6%, $p = 0.033$) and DFS (5-year DFS rate: 41.6% versus 25.0%, $p = 0.020$). No significant difference was observed when nN3 was compared with either the nN1 or nN2 subgroup ($p = 0.375$ and 0.759, respectively) (Figures 6*A*, *B*). The survival curves for OS and DFS showed distinct differences between the nN categories when pN2 patients were subdivided into different nN subgroups (5-year OS rate for nN1, nN2, and nN3 subgroup was 72.0%, 45.6%, and 19.4%, respectively, $p < 0.001$; 5-year DFS rate was 48.0%, 23.0%, and 3.9%, respectively, $p < 0.001$) (Figures 6*C*, *D*).

Each nN category was subdivided into pN1 and pN2 subgroups, and no significant difference in OS or DFS was observed between the pN1 and pN2 subgroups (Figures 7*A–F*).

In a Cox regression analysis, the nN category was identified as an independent prognostic factor for OS and DFS (versus nN3, the hazard ratios [HR] of nN0, nN1, and nN2 for OS were 0.123, 0.347, and 0.536 respectively, $p < 0.001$ for all of them; for DFS, the values were 0.088, 0.333, and 0.543, respectively, $p < 0.001$ for all of them) (Table 3). The HR of pN1 versus pN2 was not significant for OS (HR 0.729, $p = 0.081$) and was just narrowly significant for DFS (HR 0.760, $p = 0.041$) (Table 4). The HR of pN0 versus pN2 for OS and DFS were significant (0.222 and 0.173, respectively, $p < 0.001$ for both).

DISCUSSION

The TNM stage classification was developed to provide high specificity for patients with a similar prognosis and treatment options. As an essential component of this classification, nodal involvement was considered to be one of the

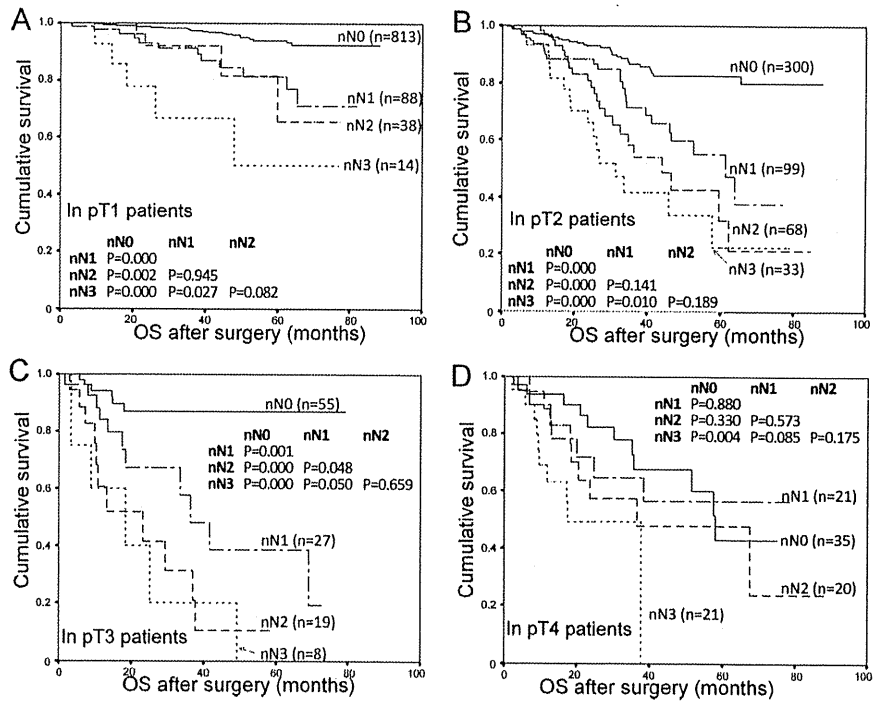

FIGURE 5. Overall survival (OS) curves according to nN category across each pT stage. *A*, OS curves according to nN category in pT1 patients. Five-year OS rate for nN0, nN1, nN2, and nN3 was 94.1%, 81.5%, 65.5%, and 50.1%, respectively. *B*, OS curves according to nN category in pT2 patients. Five-year OS rate for nN0, nN1, nN2, and nN3 was 82.6%, 55.0%, 31.9%, and 22.3%, respectively. *C*, OS curves according to nN category in pT3 patients. Five-year OS rate for nN0, nN1, nN2, and nN3 was 87.04%, 38.5%, 10.4% and 0%, respectively. *D*, OS curves according to nN category in pT3 patients. Five-year OS rate for nN0, nN1, nN2, and nN3 was 43.0%, 56.6%, 47.8%, and 0%, respectively.

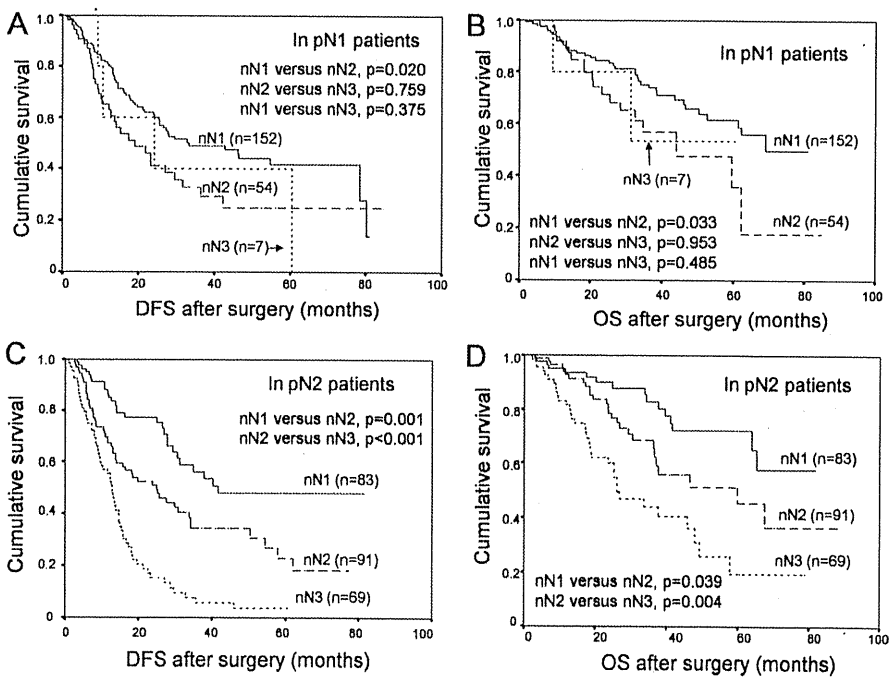

FIGURE 6. Disease-free survival (DFS) and overall survival (OS) according to nN subgroup when pN1 and pN2 patients were subdivided into different nN subgroups. *A*, DFS curves according to nN subgroup in pN1 patients. Five-year DFS rate for nN1, nN2, and nN3 subgroup was 41.6%, 25.0%, and 40%, respectively. *B*, OS curves according to nN subgroup in pN1 patients. Five-year OS rate for nN1, nN2, and nN3 subgroup was 61.5%, 35.6%, and 53.3%, respectively. *C*, DFS curves according to nN subgroup in pN2 patients. Five-year DFS rate for nN1, nN2, and nN3 subgroup was 48.0%, 23.0%, and 3.9%, respectively. *D*, OS curves according to nN subgroup in pN2 patients. Five-year OS rate for nN1, nN2, and nN3 subgroup was 72.0%, 45.6%, and 19.4%, respectively.

most important prognostic factors that influenced the survival of patients after surgery for primary NSCLC. The latest TNM staging system for lung cancer included notable changes in the T and M descriptors and the nodal map. However, the N descriptor remained the same as that in the sixth edition and depended solely on the anatomic extent of lymph node involvement.[1]

The location-based pN classification has some unsatisfactory aspects. The most important of these is the heterogeneity of pN1 and pN2 with regard to prognosis, which has been well documented, and subclassifications have been proposed.[2–13] In addition, differences among surgeons in the labeling of lymph node stations during surgery will always occur despite the introduction of a new nodal map. For

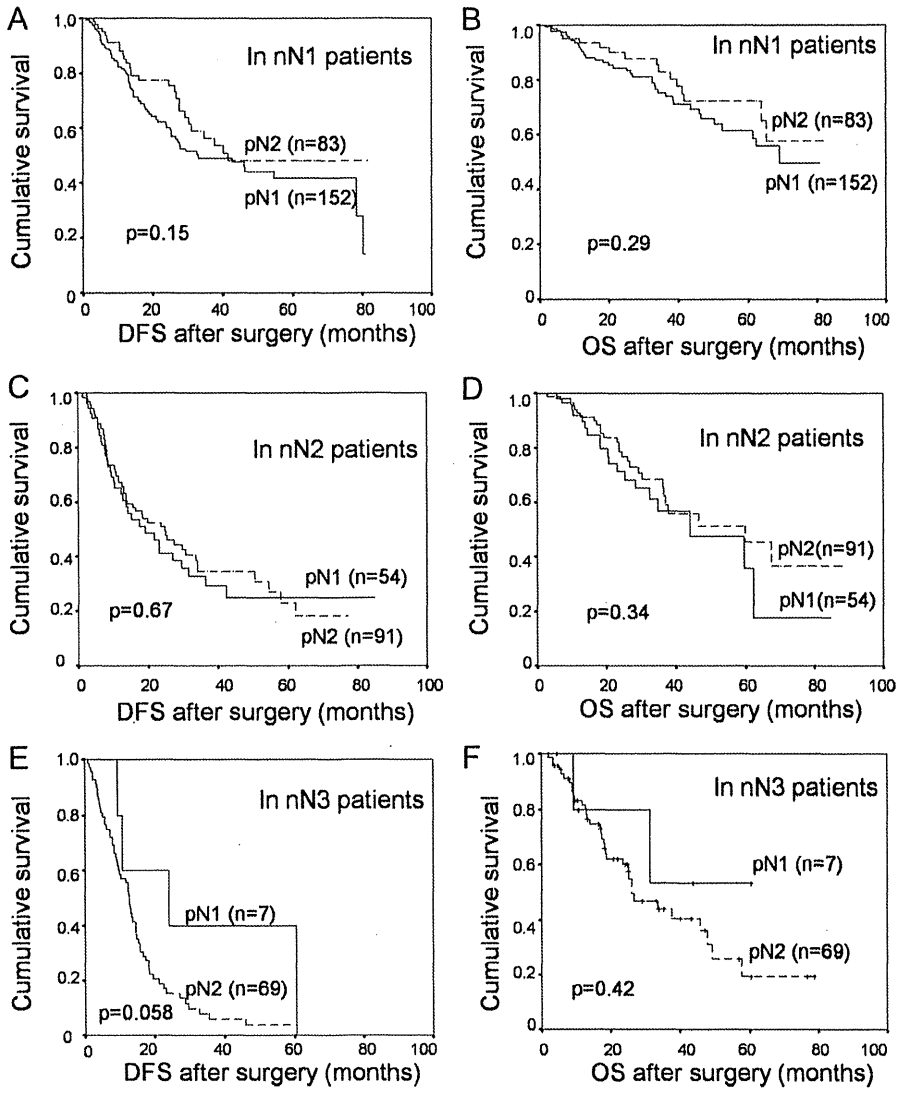

FIGURE 7. Disease-free survival (DFS) and overall survival (OS) according to pN subgroup when nN1, nN2, and nN3 patients were subdivided into pN1 and pN2 subgroups. *A*, DFS curves according to pN subgroup in nN1 patients. Five-year DFS rate for pN1 and pN2 subgroup was 41.6% and 48.0%, respectively. *B*, OS curves according to pN subgroup in nN1 patients. Five-year OS rate for pN1 and pN2 subgroup was 61.5% and 72.0%, respectively. *C*, DFS curves according to pN subgroup in nN2 patients. Five-year DFS rate for pN1 and pN2 subgroup was 25.5% and 23.0%, respectively. *D*, OS curves according to pN subgroup in nN2 patients. Five-year OS rate for pN1 and pN2 subgroup was 35.6% and 45.6%, respectively. *E*, DFS curves according to pN subgroup in nN3 patients. Five-year DFS rate for pN1 and pN2 subgroup was 40.0% and 3.9%, respectively. *F*, OS curves according to pN subgroup in nN3 patients. Five-year OS rate for pN1 and pN2 subgroup was 53.3% and 19.4%, respectively.

example, if a lymph node is located on the border between stations 4 and 10 during an operation, the same lymph node may be labeled as either N1 or N2 by different surgeons. Therefore, it is necessary to develop a refined nodal category that is simple and easy to use to provide more accurate prognostic stratifications.

In the TNM classification for some other tumors, such as gastric, breast, and colorectal cancer, the number of positive lymph nodes has been considered in the definition of pN categories.[14] In recent years, the association between the number of metastatic lymph nodes and the prognosis in resected NSCLC has also been explored. Lee et al.[15] demonstrated a stepwise deterioration with an increase in the number of positive nodes. Excellent agreement was observed between the pN and nN categories. In another study by Fukui et al.,[9] the number category defined in their study was shown to be an independent prognostic factor that could be used to stratify pN2 patients into homogenous subgroups. However, neither of these studies determined whether the pN stage classification or the nN category is the better prognostic factor. In this study, we retrospectively explored the association between the number of metastatic lymph nodes and the prognosis in 1659 resected NSCLC patients and compared the results with the classic pN stage.

In our series, although there was a significant difference in DFS between pN1 and pN2, the OS curves for the two categories were close to each other, and no significant difference was observed ($p = 0.245$). A multivariate analysis demonstrated similar results. These results implied that the pN classification had poor discriminative ability with regard to the prognosis in patients with lymph node metastasis and were very different from the report by Fukui et al.[9] and other prior reports.[11,19] While the reason for this difference is unclear, it is notable that the 5-year OS rate of pN2 patients in our study was 47.8%, which was much higher than that in prior reports[9,11] and close to that for pN1. This result might be due to the fact that all the pN2 patients who underwent surgery in this study were mN2 disease (N2-positive based

TABLE 3. Multivariate Analysis of OS and DFS Including nN Category

	OS			DFS		
Variable	**Hazard Ratio**	**95% CI**	***p***	**Hazard Ratio**	**95% CI**	***p***
Gender	0.621	0.449–0.859	0.004	—	—	—
Age	1.014	0.998–1.029	0.083	1.013	1.002–1.024	0.025
Surgical procedure (reference: wedge resection/segmentectomy)						
Lobectomy	—	—	—	0.530	0.320–0.877	0.013
Bilobectomy	—	—	—	0.465	0.244–0.887	0.020
Pneumonectomy	—	—	—	0.609	0.328–1.131	0.116
Surgical margin	1.838	1.251–2.699	0.002	1.585	1.153–2.179	0.005
Histological type (reference: adenocarcinoma)						
Squamous cell carcinoma	1.200	0.852–1.691	0.297	0.755	0.569–1.002	0.052
Large cell carcinoma	1.625	0.881–2.997	0.120	1.759	1.093–2.832	0.020
Adenosquamous carcinoma	3.386	1.616–7.097	0.001	2.528	1.271–5.029	0.008
pT stage (reference: pT1)						
pT2	2.676	1.841–3.890	<0.001	2.257	1.742–2.923	<0.001
pT3	4.571	2.842–7.350	<0.001	3.966	2.745–5.732	<0.001
pT4	4.556	2.861–7.257	<0.001	4.032	2.888–5.627	<0.001
nN category (reference: nN3)						
nN0	0.123	0.080–0.191	<0.001	0.088	0.063–0.125	<0.001
nN1	0.347	0.222–0.542	<0.001	0.333	0.237–0.468	<0.001
nN2	0.536	0.343–0.836	<0.001	0.543	0.389–0.759	<0.001

OS, overall survival; DFS, disease-free survival; nN, number of metastatic lymph nodes; CI, confidence interval.

TABLE 4. Multivariate Analysis of OS and DFS Including pN Stage

	OS			DFS		
Variable	**Hazard Ratio**	**95% CI**	***p***	**Hazard Ratio**	**95% CI**	***p***
Gender	0.673	0.486–0.932	0.017	—	—	—
Age	1.013	0.998–1.029	0.092	1.012	1.001–1.024	0.030
Surgical procedure (reference: wedge resection/segmentectomy)						
Lobectomy	—	—	—	0.548	0.331–0.905	0.019
Bilobectomy	—	—	—	0.557	0.294–1.056	0.073
Pneumonectomy	—	—	—	0.754	0.409–1.388	0.364
Surgical margin	2.141	1.470–3.118	<0.001	1.858	1.363–2.533	<0.001
Histological type (reference: adenocarcinoma)						
Squamous cell carcinoma	1.148	0.815–1.617	0.429	0.700	0.529–0.927	0.013
Large cell carcinoma	1.620	0.874–3.003	0.126	1.808	1.123–2.910	0.015
Adenosquamous carcinoma	3.609	1.725–7.547	0.001	2.498	1.259–4.954	0.009
pT stage (reference: pT1)						
pT2	2.880	1.989–4.171	<0.001	2.359	1.824–3.050	<0.001
pT3	4.529	2.811–7.298	<0.001	3.769	2.609–5.444	<0.001
pT4	4.714	2.962–7.503	<0.001	4.175	2.994–5.821	<0.001
pN stage (reference: pN2)						
pN0	0.222	0.156–0.315	<0.001	0.173	0.133–0.226	<0.001
pN1	0.729	0.512–1.040	0.081	0.760	0.583–0.989	0.041

OS, overall survival; DFS, disease-free survival; CI, confidence interval.

solely on a postoperative pathologic examination), and the exclusion criteria of cN2 disease was much stricter than that set by Fukui et al., who excluded only bulky N2 disease with extranodal invasion,[9] which resulted in a higher percentage and lower 5-year survival of pN2 population in their series than in ours (versus ours: 22% versus 14.6% and 40% versus